European Journal of Medicinal Chemistry 183 (2019) 111734

Contents lists available at ScienceDirect

European Journal of Medicinal Chemistry

journal homepage: http://www.elsevier.com/locate/ejmech

Research paper

Discovery of 2-aminopyridines bearing a pyridone moiety as potent ALK inhibitors to overcome the crizotinib-resistant mutants

Wenteng Chen [1], Xiao Guo [1], Can Zhang, Di Ke, Guolin Zhang*, Yongping Yu**

Zhejiang Province Key Laboratory of Anti-Cancer Research, College of Pharmaceutical Sciences, Zhejiang University, 310058, China

ARTICLE INFO

Article history:
Received 26 June 2019
Received in revised form
22 September 2019
Accepted 23 September 2019
Available online 24 September 2019

Keywords:
ALK inhibitors
Crizotinib-resistance
Solvent-front mutation
Pyridone
Linker

ABSTRACT

Despite the initial benefit demonstrated in clinical setting with ALK inhibitors, the challenging resistant mutants (F1174L, L1196M and G1202R) invariably developed. In this work, a series of 2-aminopyridine derivatives were designed and synthesized by C-5 position incorporation of a 2-pyridone moiety and bioisosteric replacement of the C-3 position linkers. Optimization of the 2-aminopyridine derivatives led to the identification of hit **18d** displaying a significant growth inhibition against a variety of ALK-addicted cancer cells. Especially in the case of ALK-positive Karpas-299 cell, **18d** exhibited excellent anti-proliferative potency with an IC_{50} value of about 40 nM. Moreover, **18d** demonstrated encouraging activities against wild-type ALK (19 nM), ROS1 (2.3 nM) as well as challenging crizotinib-resistant ALK^{L1196M} and ALK^{G1202R} mutants with IC_{50} values of 45 nM and 22 nM, respectively. Additionally flow cytometric analysis indicates that **18d** inhibited Karpas-299 cell viability *via* G1 phase arrest. Taken together, this work provided a promising ALK inhibitor to circumvent the clinical crizotinib-resistant mutants.

1. Introduction

Anaplastic lymphoma kinase (ALK) is a transmembrane receptor tyrosine kinase (RTK) belonging to the insulin receptor superfamily [1]. Deregulation of ALK gene is involved in the carcinogenesis process of various human cancers such as anaplastic large cell lymphomas (ALCL) [2], non-small cell lung cancer (NSCLC) [3], neuroblastoma [4] and inflammatory myofibroblastic tumors (IMT) [5], frequently in the forms of fusion with other oncogenes (NMP, EML4, TIM, etc) [6], mutation [7], gene amplification [8,9] or protein overexpression [10]. Hence, ALK becomes a promising drug target for cancer therapy [11,12]. To date, a respectable number of small molecule inhibitors were approved for modulating ALK activity. Despite the demonstrated clinical efficacy of 1st generation ALK inhibitor crizotinib (**1** , Pfizer) for the treatment of advanced NSCLC, patients develop disease relapse within one year post-treatment [13]. The short-lived clinical outcome is partly due to emergence of point mutations within the ALK kinase domain (F1174L, F1174C, L1196M, G1202R, etc) [14–17]. The recently approved next generation of ALK inhibitors, ceritinib (**2**, Novartis) [18–20], brigatinib (**3**, Takeda) [21–24], alectinib (**4**, Roche) [25–27] and lorlatinib (**5**, Pfizer) [28–30] exhibited a promising clinical efficacy against the crizotinib-resistant mutants including the gatekeeper mutation L1196M. However, the frequency of the G1202R mutation was found an increase to 21–43% in patients during the treatment of two already launched inhibitors, alectinib and ceritinib [31]. Therefore, there is still room to develop new ALK inhibitors, particularly ones capable of combating the challenging L1196M and G1202R mutations (see Fig. 1).

Generally, many currently available ALK inhibitors are ATP-competitive type I TKIs, which feature an ATP adenine equivalent kinase hinge binder with Met^{1199} and Glu^{1197}. Additionally, an aryl fragment extended into the inside hydrophobic pocket, a functional linker for conformational interaction with the gate-keeper and an extra motif extended to the solvent area [32–34]. We conducted a molecular modeling on crizotinib with $ALK^{G1202R/L1196M}$ by incorporating the Arg^{1202} mutation using ALK^{L1196M} -crizotinib co-crystal structure (PDB 2YFX) as a template [32]. As shown in Fig. 2A, the solvent-exposure motif of crizotinib sits atop and in close proximity to the residue Arg^{1202}, which possibly accounts for the moderate potency of crizotinib on G1202R mutation. Thus, it is questioned whether the exploration of a new "tail" for the solvent-front region might give rise to new inhibitors for combating

* Corresponding author.
** Corresponding author.
E-mail addresses: guolinzhang@zju.edu.cn (G. Zhang), yyu@zju.edu.cn (Y. Yu).
[1] These two authors contributed equally to this work.

https://doi.org/10.1016/j.ejmech.2019.111734
0223-5234/

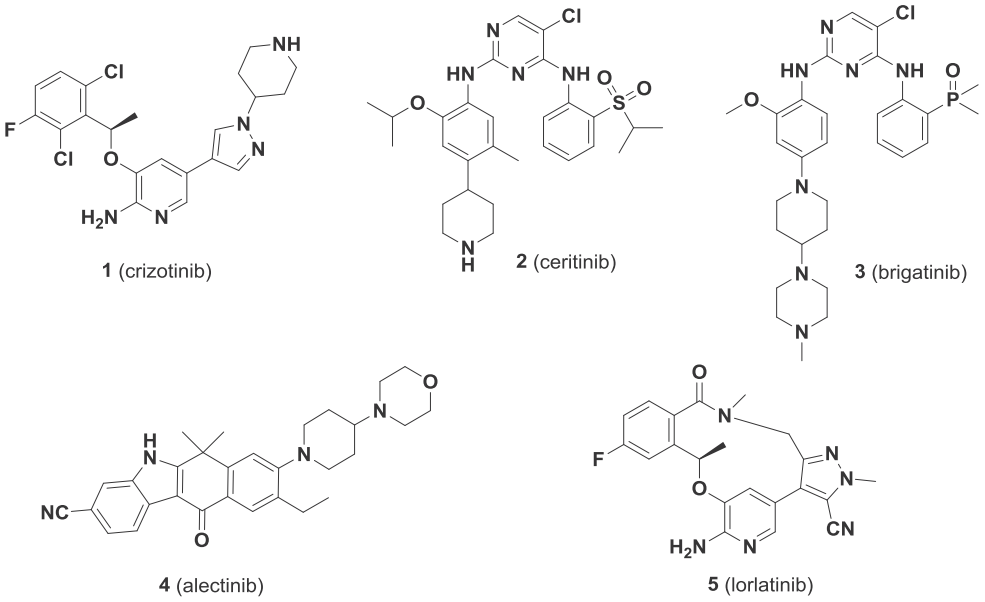

Fig. 1. The structure of ALK inhibitors in clinic.

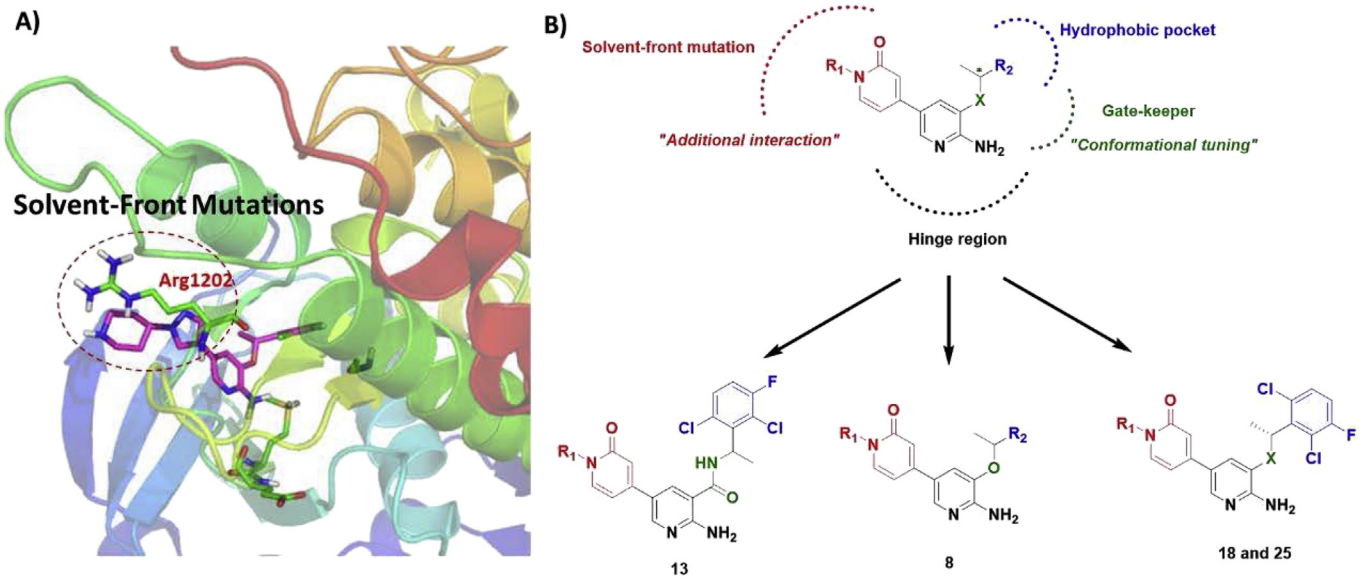

Fig. 2. Design strategies for target compounds. (A) Binding conformation of crizotinib with ALK $^{G1202R/L1196M}$. (B) The design of new ALK inhibitor analogues with pyridone moiety.

solvent-front mutation ALK^{G1202R}. Based on this hypothesis, a new "tail" pyridone motif was designed and proposed to trigger additional interaction with the solvent-front mutation G1202R (Fig. 2B, analogue 8). Furthermore, the linkers at the C-3 position of the 2-aminopyridine core were also investigated. A flexible sp^3 (*O*-linker and S-linker, analogue 18 and 25) and rigid sp^2 (amide-linker, analogue **13**) were designed for the compatibility of conformational tuning the inhibitors and gate-keeper mutation L1196M.

2. Results and discussion

2.1. Chemistry

The synthesis commenced with hydrolysis of 2-amino-4-bromopyridine **1**, followed by substitution with various commercially available alkyl halides, to give the intermediates **3** as shown in Scheme 1. The benzyl alcohol derivatives **4** were easily converted to ether derivatives **5** using classical Mitsunobu coupling [34]. Chemo-selective reduction of the nitro group with iron and acetic acid (HOAc) afforded amine **6**, and regioselective bromination gave the desired product **7** [35,36]. Then palladium-catalyzed boronation of **7** followed by a sequential Suzuki coupling with aryl bromides **2** or **3** delivered compounds **8a**-**8l**.

The construction of 2-amino-5-bromo-N-(1-(2, 6-dichloro-3-fluorophenyl) ethyl) nicotinamide **12** began with 1-(2, 6-dichloro-3-fluorophenyl) ethan-1-ol **4d**, as presented in Scheme 2. The mesylate **9** was easily obtained from benzyl alcohol **4d** *via* MsCl protection [37]. Substitution of **9** with sodium azide, followed by reduction of the resulting azides with Zn/NH_4Cl [38], gave the desired amine **11**. Condensation of amine **11** with 2-amino-5-

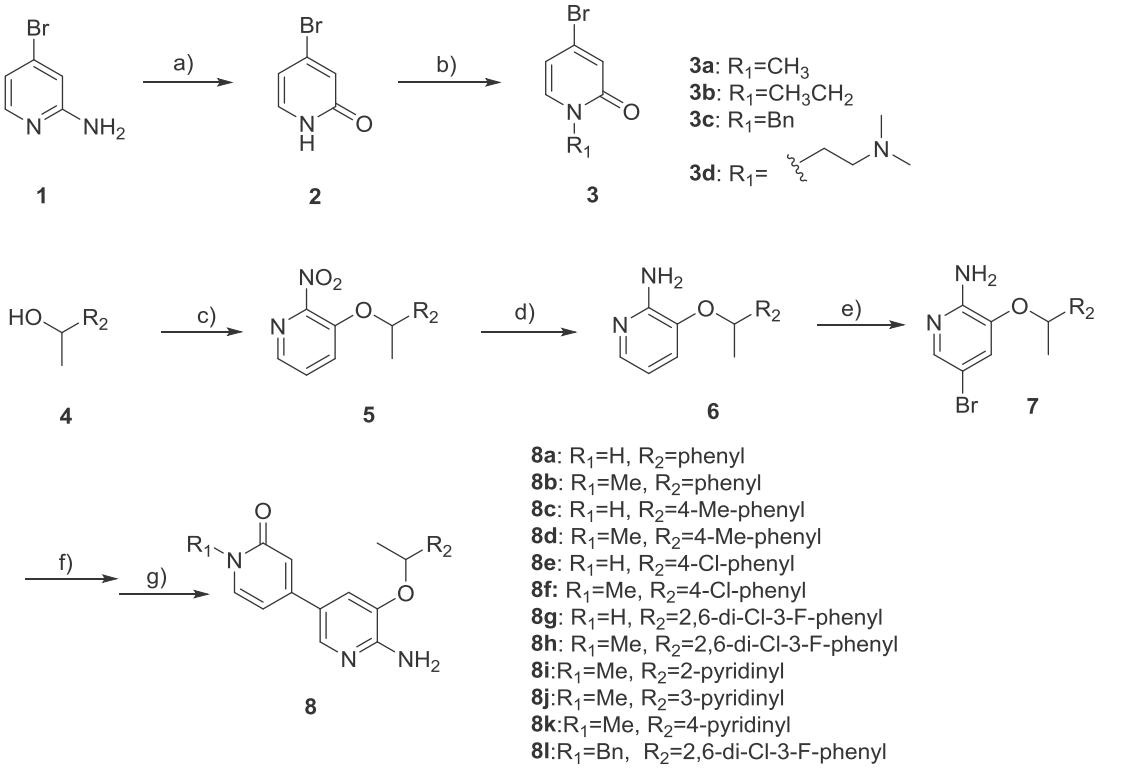

Reagents and conditions: a) $NaNO_2$, H_2SO_4, 0 °C, 3 h; b) R_1I or R_1 Br, K_2CO_3, acetone, 60 °C, 24 h or R_1Cl, KOH, DMSO, 40 °C, 1 h; c) 2-nitropyridin-3-ol, PPh_3, DEAD, THF, 0 °C, 4 h; d) Fe, HOAC, EtOH, reflux, 1 h; e) NBS, CH_3CN, 0 °C,15 min; f) 4,4,4',4',5,5,5',5'-octamethyl-2,2'-bi(1,3,2-dioxaborolane), $Pd(dppf)Cl_2$, KOAC, Dioxane,110 °C, 8 h; g) 2 or 3, $Pd(dppf)Cl_2$, Cs_2CO_3, Dioxane,110 °C, 10 h.

Scheme 1. Synthesis of compounds **8a-8l**.

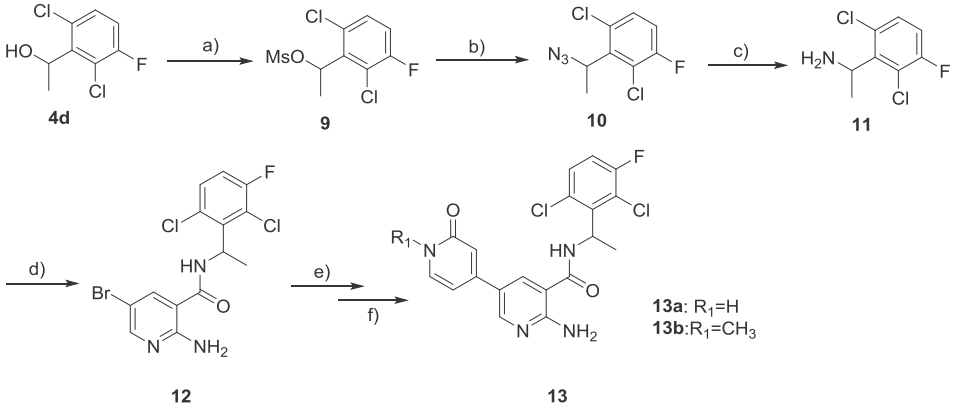

Reagents and conditions: a) MsCl, Et_3N, DCM, 0 °C-rt, 10 h; b) NaN_3, DMF, 50 °C, 8 h ; c) Zn, NH_4Cl, EtOH-H_2O (3:1), rt, 3 h; d)2-amino-5-bromonicotinic acid, HATU, DIPEA, DMF, 0 °C-rt, 8 h; e) 4,4,4',4',5,5,5',5'-octamethyl-2,2'-bi(1,3,2-dioxaborolane), $Pd(dppf)Cl_2$, KOAC, Dioxane,110 °C, 8 h; f) 2 or 3, $Pd(dppf)Cl_2$, Cs_2CO_3, Dioxane,110 °C, 10 h.

Scheme 2. Synthesis of compounds **13a-13b**.

bromonicotinic acid delivered the amide **12**. Next, introduction of the pyridone fragments **2** or **3** at the C-5 position of **12** was achieved by similar Suzuki coupling shown in Scheme 1. Compound **12** was subsequently transformed to products **13a-13b**.

The chiral enantiomer **18a-18g** were similarly obtained as shown in Scheme 1 And (*S*)-1-(2, 6-dichloro-3-fluorophenyl) ethan-1-ol **14** was utilized as the alternative starting material. A Mitsunobu reaction of chiral alcohol (*S*)-**14** and 3-hydroxy-2-nitropyridine proceeded in good yield with complete inversion of stereochemistry to give the desired ether (*R*)-**15** [35]. Similarly, subsequent chemo-selective reduction of the nitro group and region-selective bromination gave the key intermediate **17** [35,36].

Finally, treatment of **17** with aryl bromides **2** or **3** under Suzuki coupling conditions furnished the desired products **18a-18g** (Scheme 3).

Compared to the ether **5** and **15**, the thioether **22** was not obtained from 2-nitropyridine-3-thiol *via* conventional Mitsunobu reaction. As shown in Scheme 4, intermediate **22** was obtained *via* hydrolysis of the dimethylcarbamothioate **21** followed by a sequential substitution with mesylate **19** [37,39]. And the dimethylcarbamothioate **21** was prepared from 3-hydroxyl-2-nitropyridine with dimethylthiocarbamoyl chloride and DABCO in DMF following with a tautomerism [37]. Next, reduction of the nitro group and bromination of **23** delivered key intermediate **24**. Compound **24** was subsequently transformed to target products **25a-25d** in a similar manner as described in Scheme 1.

2.2. Biological evaluation

2.2.1. In vitro inhibitory activities against ALK-dependent cancer cells

Activities of target compounds (**8a-8l**, **13a-13b**, **18a-18g** and **25a-25d**) against tumor cells expressing NMP-ALK are demonstrated in ALCL cell Karpas-299 (Tables 1–3).

In order to identify potent ALK inhibitors, we initially selected pyridin-2(1*H*)-one at C-5 position and retained the oxygen as a linker while varying the aryl fragment (R_2 part). As shown in Table 1, the incorporation of phenyl (**8a**), 4-methylphenyl (**8c**), 4-chlorophenyl (**8e**), 2-pyridinyl (**8i**), 3-pyridinyl (**8j**) and 4-pyridinyl (**8l**) as the R_2 substitution resulted in a significant loss of activity. While the 2, 6-dichloro-3-fluorophenyl substitution (**8g**, 0.12 μM) is tolerated with a comparable IC_{50} value to crizotinib (0.03 μM). This indicated that 2, 6-dichloro-3-fluorophenyl group would be beneficial for a hydrophobic interaction. The activities did not significantly change with the introduction of methyl (**8h**, 0.20 μM) or benzyl (**8l**, 0.32 μM) as R_1 substitutions. However, simply replacing the *O*-linker with another rigid amide-linker (**13**) caused a complete loss of activity. **13a** and **13b** displayed no activity up to 20 μM, suggesting that the rigidity of the amide-linker would be detrimental for the interaction with the target protein.

With the expectation of an improvement in potency, 2, 6-dichloro-3-fluorophenyl group was kept as the R_2 substituent while the stereochemistry of the *O*-linker and modification on the N-position of pyridone ring (R_1 part) were further investigated. The results are shown in Table 2. Compared to the racemates (**8g**, **8h** and **8l**), the corresponding *R*-enantiomers **18a-18c** displayed 2- to 5- fold more activity against Karpas-299 (**8g** *vs* **18a**, **8h** *vs* **18b** and **8l** *vs* **18c**). The encouraging results suggested the *R*-configuration is more effective in affecting the proliferation of Karpas-299. Appending alkanes at the N-position of pyridone rings (**18b**, **18e-18g**) displayed good tolerance in anti-proliferative activities (0.04–0.21 μM), albeit the carbon chain length slightly decreased the cellular potency. Moreover, incorporation of basic substitution (N, N-dimethylethyl, **18d**) displayed more effective potency and the IC_{50} value reached to 0.04 μM, while introducing a bulky benzyl group resulted in a slight decrease in potency (**18c**, $IC_{50} = 0.13$ μM). In consideration of bio-isosteres, a S-linker was also evaluated. However, the compounds with a S-linker (**25a-25d**) exhibited moderate anti-proliferative activities even with the N, N-dimethylethyl group (**25d**, $IC_{50} = 0.28$ μM). It therefore appears in this case the *O*-linker is more favor for the cellular potency.

Givin their promising anti-proliferactive activities against Karpas-299, **18a-18g** were selected for further evaluation in other ALK-addicted cancer cells, including ALCL (Karpas-299 (NPM-ALK)), neuroblastoma (SH-SY5Y (F1174L), SK-N-BE2 (wt)) and NSCLC (NCI–H2228 (EML4-ALK)). The results are summerized in Table 3, most of the compounds displayed moderate to high potency across the entire panel of these ALK-addicted cell lines. This likely reflects that anti-proliferative activity of compound **18** is "on-target" to ALK.

2.2.2. In vitro inhibitory activities against ALK wild type and resistant mutants

Based on the SAR above, **18a-18e** with representative structural divesity were chosen for further evaluation. As shown in Table 4, **18a-18e** showed good ALK^{WT} potency that is consistent with the potency against the ALK-addicited cancer cells. Next, their inhibitory activities against the most common and challenging crizotinib-resistant mutants including gatekeeper mutation L1196M and solvent-front mutant G1202R were tested. Compared to crizotinib

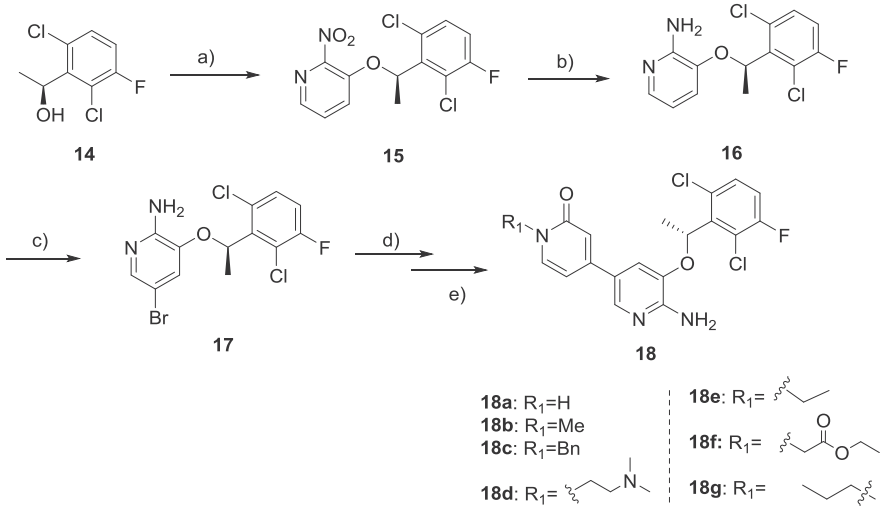

Reagents and conditions: a) 2-nitropyridin-3-ol, PPh_3, DEAD, THF, 0 °C, 4 h; b) Fe, HOAC, EtOH, reflux, 1 h; c) NBS, CH_3CN, 0 °C,15 min;d) 4,4,4',4',5,5,5',5'-octamethyl-2,2'-bi(1,3,2-dioxaborolane), $Pd(dppf)Cl_2$, KOAC, Dioxane,110 °C, 8 h; e) **2** or **3**, $Pd(dppf)Cl_2$, Cs_2CO_3, Dioxane,110 °C, 10 h.

Scheme 3. Synthesis of compounds **18a-18g**.

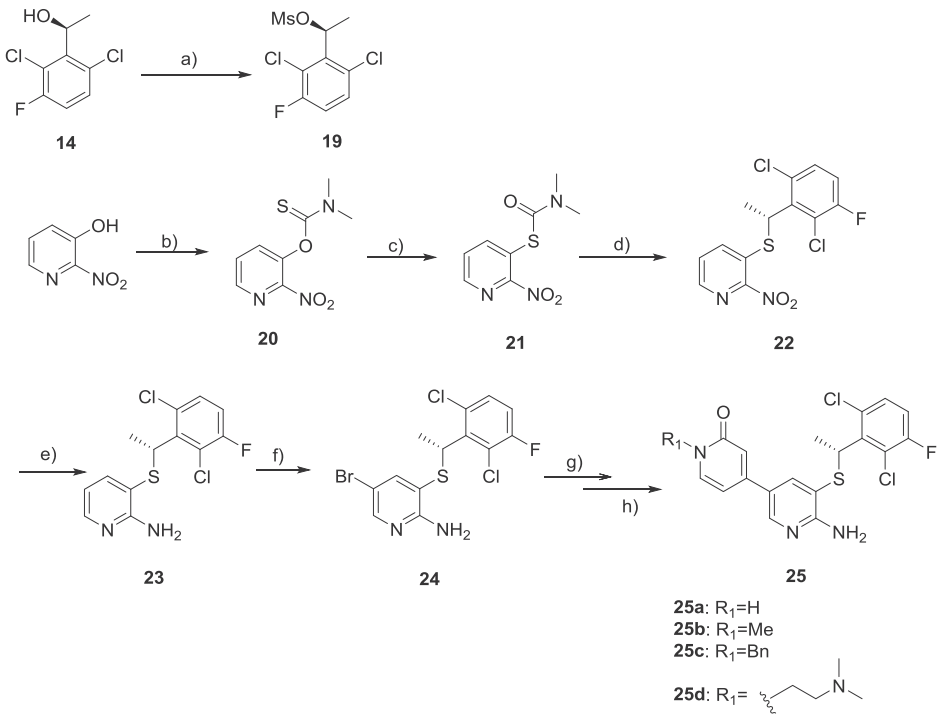

Reagents and conditions: a) MsCl, Et_3N, DCM, 0 °C-rt, 10 h; b) dimethylcarbamothioic chloride, DABCO, DMF, rt, 24 h; c) Ph_2O, 160 °C , 3 h; d) **19**, KOH, MeOH/THF/H_2O (2:1:1), 0 °C-rt; e) Fe/HCl, EtOH, reflux; f) Br_2, K_2CO_3, DCM, 0 °C; g) 4,4,4',4',5,5,5',5'-octamethyl-2,2'-bi(1,3,2-dioxaborolane), Pd(dppf)Cl_2, KOAc, Dioxane, 80°C,8h; h) **2** or **3**, Pd(dppf)Cl_2, Cs_2CO_3, Dioxane,110 °C,10h.

Scheme 4. Synthesis of compounds **25a-25d**.

(IC_{50} = 366 nM), **18a**, **18b** and **18d** showed excellent inhibitory potencies against the crizotinib-resistant mutation ALK^{L1196M} with IC_{50} values of 66, 85 and 45 nM, respectively. Notably, **18d** exhibited excellent inhibitory activity with a competitive IC_{50} value (22 nM) against ALK^{G1202R}, the most refractory mutation accounting for drug resistance of the 2nd generation ALK inhibitors. Additionally, **18d** displayed an excellent effect against ROS1 (2.3 nM). These indicated **18d** might be a promising ALK/ROS1 inhibitor for overcoming the clinical crizotinib-resistant mutants.

2.2.3. 18d induces G1-phase cell cycle arrest in Karpas-299 cell

To better understand the possible mechanism associated with anti-proliferative activity, the effect of **18d** on the cell cycle distribution in Karpas-299 was explored. After cells were treated with vehicle or 1 μM of **18d** for 48 h, DNA content in the control group displayed a typical histogram observed in exponentially growing cells, while **18d** induced G1-phase cell cycle arrest in Karpas-299 (81.5%). (Fig. 3). This result indicated that the cell cycle arrest contributed to the anti-proliferative activity of **18d**.

2.3. Molecular docking

In order to better understand the binding mode, molecular docking model of **18d** were performed based upon the cocrystal structure of ALK^{L1196M} with crizotinib (PDB 2YFX). As shown in Fig. 4A, **18d** occupies the kinase domain in a similar manner to crizotinib. Interestingly, the basic "tail", 1-(2-(dimethylamino) ethyl)pyridine-2(1*H*)-one moiety, was engaged in hydrogen bond interactions with Asp1203 and Ser1206/Gly1202, possibly validating our hypothesis. Furthermore, in the G1202R/L1196M mutant model (Fig. 4B), the"tail" of **18d** was involved in a hydrogen bond with Arg1202, which possibly explains the potency of **18d** to overcome G1202R mutant.

3. Conclusion

The emergence of on-target kinase domain mutations (L1196M) and solvent-front mutations (G1202R) are among the most recalcitrant of crizotinib-resistance. Based on the built $ALK^{L1196M/G1202R}$ model, the piperidinyl-pyrzaole ring of crizotinib was altered with a new 2-pyridone motif as well as a flexible sp^3 (S-linker) and rigid sp^2 (amide-linker) functionalities were introduced to replace the known *O*-linker. Optimization of 2-aminopyridine derivatives led to the identification of hit **18d**. **18d** displayed remarkable anti-proliferative potencies against ALK-addicted cancer cell lines with the IC_{50} values ranging from 0.04 μM to 1.67 μM. Moreover, **18d** exhibited encouraging activities against the most common gatekeeper mutant L1196M (45 nM), the challenging resistant mutant G1202R (22 nM) and ROS1 (2.3 nM), which are superior to crizotinib. Additionally, **18d** inhibited Karpas-299 cell viability *via* G1 phase arrest. These findings show that **18d** would be a promising ALK inhibitor for overcoming the clinical crizotinib-resistant mutants.

4. Experimental section

4.1. Chemistry

Unless otherwise noted, all solvents and chemicals were used as purchased without further purification. Purity of all final compounds was 95% or higher. All reported yields are isolated yields after column chromatography. ^1H NMR spectra were recorded on a

Table 1
In vitro anti-proliferative activities of compound **8** and **13**.

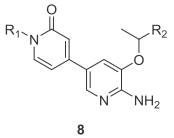

8

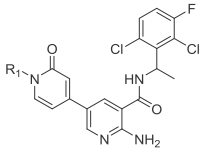

13

Compound	R_1	R_2	Karpass299 IC_{50}/μM[a]
8a	H		4.40 ± 0.29
8b	CH_3		2.86 ± 0.24
8c	H		10.17 ± 1.39
8d	CH_3		7.78 ± 0.20
8e	H		17.80 ± 1.28
8f	CH_3		20.92 ± 1.41
8g	H		0.12 ± 0.004
8h	CH_3		0.20 ± 0.05
8i	CH_3		11.91 ± 0.08
8j	CH_3		11.17 ± 1.12
8k	CH_3		>20
8l	Bn	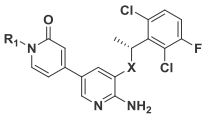	0.32 ± 0.19
13a	H	—	>20
13b	CH_3	—	>20
crizotinib	—	—	0.03 ± 0.004

[a] The inhibitory effects of individual compounds on the proliferation of cancer cell were determined by the MTT assay. The data reported are the mean values from two independent experiments.

Table 2
In vitro anti-proliferative activities of compound **18** and **25**.

Compound	R_1	X	Karpass299 $IC_{50}/\mu M$[a]
18a	H	O	0.05 ± 0.03
18b	Me	O	0.04 ± 0.00
18c	Bn	O	0.13 ± 0.01
18d		O	0.04 ± 0.01
18e		O	0.06 ± 0.01
18f		O	0.21 ± 0.06
18g		O	0.11 ± 0.01
25a	H	S	0.72 ± 0.02
25b	Me	S	0.40 ± 0.17
25c	Bn	S	0.79 ± 0.10
25d	fx21	S	0.28 ± 0.18
crizotinib	–	–	0.03 ± 0.004

Table 3
Anti-proliferative activities of selected compounds against a panel of ALK-addicted cell lines[a].

Compd.	Cell line/$IC_{50}(\mu M)$			
	Karpas-299 (NPM-ALK)	SH-SY5Y (F1174L)	SK-N-BE2 (WT)	NCI−H2228 (EML4-ALK)
18a	0.05 ± 0.03	2.07 ± 0.19	0.75 ± 0.23	0.64 ± 0.06
18b	0.04 ± 0.00	1.87 ± 0.35	0.83 ± 0.03	0.69 ± 0.05
18c	0.13 ± 0.01	1.35 ± 0.28	1.02 ± 0.08	1.30 ± 0.21
18d	0.04 ± 0.01	1.67 ± 0.25	0.71 ± 0.11	0.44 ± 0.28
18e	0.06 ± 0.01	2.51 ± 0.08	1.44 ± 0.02	1.20 ± 0.06
18f	0.21 ± 0.06	1.85 ± 0.05	1.23 ± 0.19	3.32 ± 0.28
18g	0.11 ± 0.01	2.15 ± 0.42	1.43 ± 0.01	1.22 ± 0.03
crizotinib	0.03 ± 0.004	0.85 ± 0.08	1.33 ± 0.25	0.64 ± 0.03

[a] The inhibitory effects of individual compounds on the proliferation of cancer cell lines were determined by the MTT assay. The data reported are the mean values from two independent experiments.

Table 4
Inhibitory activities of selected compounds against different status of ALKs and ROS1.[a].

Compd.	Kinase/IC_{50} (nM)			
	ALK (WT)	ALK(L1196M)	ALK(G1202R)	ROS1
18a	12	66	43	–
18b	21	85	44	–
18c	43	393	–	–
18d	19	45	22	2.3
18e	21	136	–	–
crizotinib	30	366	>500	6.5

[a] The data reported are the mean values from two duplicated wells.

Bruker DRX-500 [Bruker Biospin, Germany]. Chemical shifts are reported in ppm relative to the residual solvent peak ($CDCl_3$, TMS: 0.00). Multiplicity was indicated as follows: s (singlet); d (doublet); t (triplet); q (quartet); m (multiplet); dd (doublet of doublet); dt (triplet of doublet); td (doublet of triplet); brs (broad singlet) etc. Intermediates were purified by column chromatography on silica gel (200−300 mesh). HPLC analysis and the HRMS of all biologically evaluated compounds was confirmed on a Agilent 1290 HPLC-6224 Time of Fight Mass Spectrometer using PhenomenexLuna 5μ C18, 100 Å, 150 × 4.60 mm 5 μm column at a flow rate of 0.5 mL/min using liner gradients buffer B in A (B: CH_3OH containing 0.1% formic acid, A: H_2O containing 0.1% formic acid). Mobile phase B was increased linearly from 5% to 95% over 7 min and 95% over the next 2 min, after which the column was equilibrated to 5% for 1 min.

4.1.1. General procedure for the synthesis of 4-bromopyridin-2(1H)-one (2)

2-amino-4-bromopyridine (3.5 mmol) was dissolved in 20 mL 2M H_2SO_4 in an ice-bath. A saturated $NaNO_2$ (4.0 mmol) solution was added dropwise into the above solution. After the completion of addition overnight, the precipitate was collected for further reaction without any purification. Light yellow solid. Yield: 72%. ^1H NMR (500 MHz, $CDCl_3$) δ 13.07 (s, 1H), 7.22 (d, $J = 7.0$ Hz, 1H), 6.83 (d, $J = 1.5$ Hz, 1H), 6.46 (dd, $J = 7.0$, 2.0 Hz, 1H). HRMS (ESI) *m/z* calcd for C_5H_4BrNO $[M+H]^+$:173.9549, found: 173.9551.

*4.1.2. General procedure for the synthesis of **3***

To an ice-cold solution of 2-hydroxy-4-bromopyridine (5.75 mmol) in THF was added NaH (5.75 mmol) portion-wise. The reaction mixture was stirred in an ice-bath for 15 min followed by addition of halide or iodine (17.24 mmol). The resulting reaction mixture was stirred at room temperature for 16 h. After the completion of the reaction, 20 mL of H_2O was added and the reaction mixture was extracted with EtOAc 3 times. The combined organic layer was collected and rinsed with brine. The mixture was evaporated to obtain the crude product and purified by silica gel for **3a-3d**.

*4.1.2.1. 4-bromo-1-methylpyridin-2(1H)-one (**3a**): [40].* Yellow solid. Yield: 87%. HRMS (ESI) *m/z* calcd for C_6H_7BrNO $[M+H]^+$:187.9706, found: 187.9702.

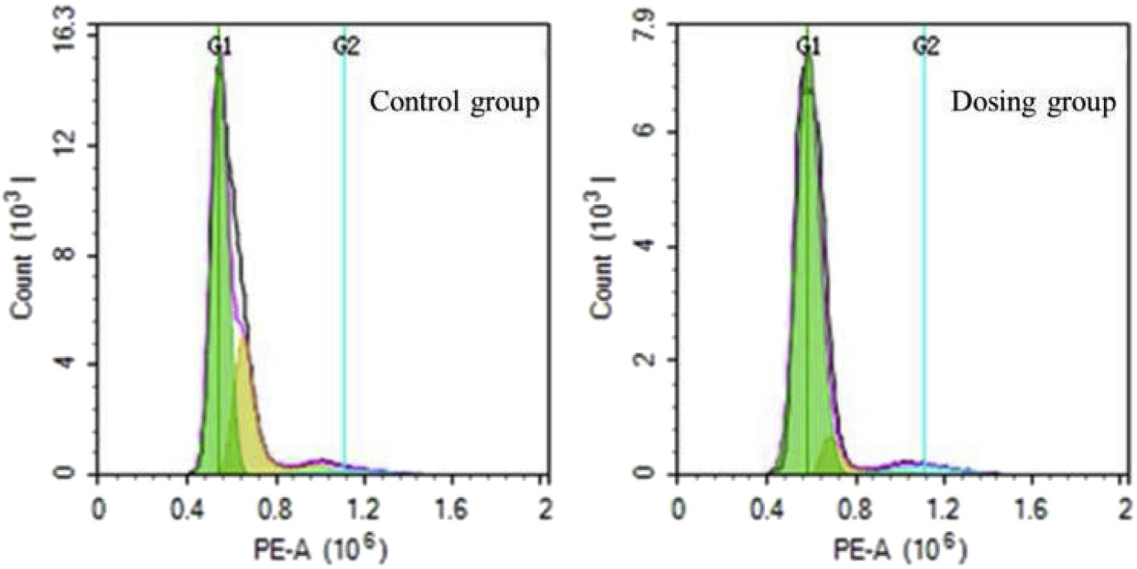

G1	S	G2
58.94	28.83	3.68

G1	S	G2
81.46	8.00	5.43

Fig. 3. Cell cycle arrest induced by **18d** in Karpas-299 cell.

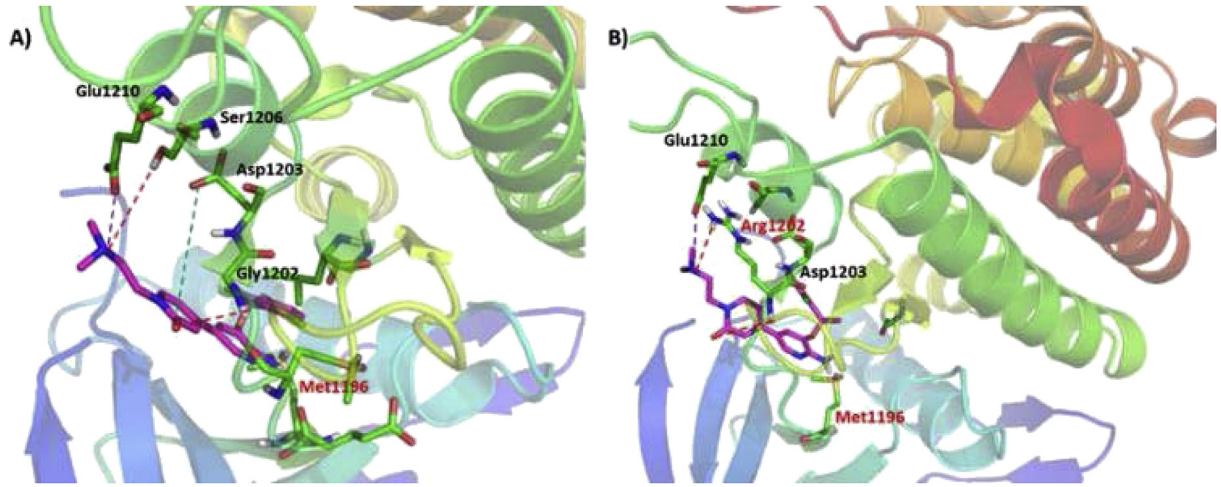

Fig. 4. The binding models of **18d** with ALK. (A) Predicted binding conformation of **18d** in the binding site cavity of ALK^{L1196M} (PDB 2YFX). (B) Predicted binding conformation of **18d** in the ATP binding site of $ALK^{G1202R/L1196M}$.

*4.1.2.2. 4-bromo-1-ethylpyridin-2(1H)-one (**3b**): [41].* Yellow solid. Yield: 81%. HRMS (ESI) *m/z* calcd for C_7H_9BrNO $[M+H]^+$: 201.9862, found: 201.9872.

*4.1.2.3. 1-benzyl-4-bromopyridin-2(1H)-one (**3c**): [41].* White solid. Yield: 65%. HRMS (ESI) *m/z* calcd for $C_{12}H_{11}BrNO$ $[M+H]^+$: 264.0019, Found:264.0026.

*4.1.2.4. 4-bromo-1-(2-(dimethylamino)ethyl)pyridin-2(1H)-one (**3d**).* White solid. Yield: 60%.^{1}H NMR (500 MHz, $CDCl_3$) δ 7.19 (d, J = 7.5 Hz, 1H), 6.80 (d, J = 2.0 Hz, 1H), 6.29 (dd, J = 7.0, 2.0 Hz, 1H), 3.96 (t, J = 6.0 Hz, 2H), 2.59 (t, J = 6.0 Hz, 2H), 2.26 (s, 6H). HRMS (ESI) *m/z* calcd for $C_9H_{14}BrN_2O$ $[M+H]^+$: 245.0284, Found: 245.0282.

*4.1.3. General procedure for the synthesis of 2-nitro-5-(1-(pyridin-2-yl)ethoxy)pyridine (**5i**)*

1-(pyridin-2-yl)ethan-1-ol (20 mmol), PPh_3 (30 mmol) and 2-nitro-3-hydroxyl pyridine (20 mmol) were dissolved in 30 mL THF under the N_2 atmosphere. When the reaction was cooled to 0 °C, DEAD (30 mmol) was added dropwise. Then the reaction was warmed to room temperature for 3 h. The reaction mixture was evaporated and crystallized by EtOH-Pet. Yellow solid. Yield: 85%.^{1}H NMR (500 MHz, DMSO-d_6) δ 8.62-8.55 (m, 1H), 8.08 (dd, J = 5.0, 1.5 Hz, 1H), 7.86-7.83 (m, 2H), 7.66 (dd, J = 8.5, 4.5 Hz, 1H), 7.45 (d, J = 8.0 Hz, 1H), 7.36-7.33 (m, 1H), 5.82 (q, J = 6.5 Hz, 1H), 1.62 (d, J = 6.5 Hz, 3H). HRMS (ESI) *m/z* calcd for $C_{12}H_{12}N_3O_3$ $[M+H]^+$: 246.0873, Found: 246.0880.

*4.1.4. General procedure for the synthesis of 5-(1-(pyridin-2-yl) ethoxy)pyridin-2-amine (**6i**)*

The **5i** (16 mmol) and Fe (48 mmol) were dissolved in 100 mL EtOH and 25 mL AcOH. The reaction was refluxed for 2 h. After the completion of the reaction, the pH was adjusted to a basic condition with Na_2CO_3 solution. The mixture was extracted with EtOAc and the combined organic layer was evaporated to get the crude product. The final product was crystallized with EtOAc/Pet. Yield: 88%. ^{1}H NMR (500 MHz, DMSO-d_6) δ 8.55-8.54 (m, 1H), 7.78 (td, J = 7.5, 1.5 Hz, 1H), 7.50 (d, J = 8.0 Hz, 1H), 7.46 (dd, J = 5.0, 1.5 Hz, 1H), 7.31-7.28 (m, 1H), 6.83 (dd, J = 8.0, 1.5 Hz, 1H), 6.35 (dd, J = 8.0, 5.0 Hz, 1H), 5.77 (s, 2H), 5.43 (q, J = 6.5 Hz, 1H), 1.60 (d, J = 6.5 Hz, 3H). HRMS (ESI) *m/z* calcd for $C_{12}H_{14}N_3O$ $[M+H]^+$: 216.1131, Found: 216.1129.

*4.1.5. General procedure for the synthesis of 3-bromo-5-(1-(pyridin-2-yl)ethoxy)pyridin-2-amine (**7i**)*

The **6i** (15 mmol) was dissolved in 50 mL MeCN and 25 mL CH_2Cl_2, NBS (15 mmol) was added to the above mixture portion-wise in an ice-bath. After the reaction was stirred for 15 min, 5 mL H_2O was added to quench the reaction. The mixture was extracted with DCM and the combined organic layer was evaporated to get the crude product. The final product was crystallized with MeOH. Yield: 78%. ^{1}H NMR (500 MHz, DMSO-d_6) δ 8.57-8.55 (m, 1H), 7.81 (td, J = 7.5, 1.5 Hz, 1H), 7.53-7.51 (m, 2H), 7.33-7.31 (m, 1H), 7.02 (d, J = 2.0 Hz, 1H), 6.07 (s, 2H), 5.51 (q, J = 6.5 Hz, 1H), 1.60 (d, J = 6.5 Hz, 3H). HRMS (ESI) *m/z* calcd for $C_{12}H_{13}BrN_3O$ $[M+H]^+$: 294.0237, Found: 294.0233.

*4.1.6. General procedure for the synthesis of **8***

To a 50 mL round-bottom flask under a nitrogen atmosphere **7** (10.0 mmol), bispinacolatodiboron (10.0 mmol), $PdCl_2(dppf)_2$ (0.5 mmol), potassium acetate (15 mmol) and 1, 4-dioxane (20 mL) were added. The reaction mixture was stirred at 80 °C for 8 h. After the completion of the reaction, Cs_2CO_3 (15 mmol), $PdCl_2(dppf)_2$ (0.5 mmol), 3 (11.0 mmol) and 0.5 mL H_2O were added to the above mixture. The reaction was stirred at 110 °C overnight. After the completion of the reaction, 20 mL of H_2O was added and the reaction mixture was extracted with DCM for 3 times. The combined organic layer was collected and rinsed with brine. The mixture was evaporated to obtain the crude product and purified by silica gel for **8a-8l**.

*4.1.6.1. 6-Amino-5-(1-phenylethoxy)-[3, 4′-bipyridin]-2′(1′H)-one (**8a**).* Grey solid; m.p. 231–233 °C; Yield: 71%. HPLC: 98.77%, t_R = 4.073 min ^{1}H NMR (500 MHz, DMSO-d_6) δ 11.39 (s, 1H), 7.85 (d, J = 1.6 Hz, 1H), 7.48 (d, J = 7.4 Hz, 2H), 7.32 (dd, J = 15.4, 7.6 Hz, 3H), 7.22 (dd, J = 15.3, 4.4 Hz, 2H), 6.37 (d, J = 4.8 Hz, 2H), 6.24 (s, 2H), 5.73 (q, J = 6.2 Hz, 1H), 1.57 (d, J = 6.3 Hz, 3H). ^{13}C NMR (500 MHz, DMSO-d_6) δ162.8, 152.5, 149.6, 142.6, 139.2, 137.4, 135.1, 128.5, 127.6, 125.9, 120.6, 115.5, 113.2, 103.0, 74.8, 23.8. HRMS (ESI) *m/z* calcd for $C_{18}H_{18}N_3O_2$ $[M+H]^+$: 308.1394, Found: 308.1394.

*4.1.6.2. 6-Amino-1′-methyl-5-(1-phenylethoxy)-[3,4′-bipyridin]-2′(1′H)-one (**8b**).* Black solid; m.p. 205–207 °C; Yield: 65%. HPLC: 100%, t_R = 4.240 min ^{1}H NMR (500 MHz, DMSO-d_6) δ 7.87 (d, J = 1.3 Hz, 1H), 7.61 (d, J = 7.1 Hz, 1H), 7.48 (d, J = 7.4 Hz, 2H), 7.32 (t, J = 7.5 Hz, 2H), 7.23 (dd, J = 8.1, 4.5 Hz, 2H), 6.47 (d, J = 1.5 Hz, 1H), 6.46-6.37 (m, 1H), 6.25 (s, 2H), 5.74 (q, J = 6.2 Hz, 1H), 3.35 (s, 3H), 1.57 (d, J = 6.3 Hz, 3H). ^{13}C NMR (500 MHz, DMSO-d_6) δ 162.1, 152.5, 148.5, 142.6, 139.3, 139.2, 137.4, 128.5, 127.6, 125.9, 120.2, 115.5, 112.2, 102.9, 74.8, 36.2, 23.8. HRMS (ESI) *m/z* calcd for $C_{19}H_{20}N_3O_2$ $[M+H]^+$: 322.1550, Found: 322.1554.

*4.1.6.3. 6-Amino-5-(1-(p-tolyl)ethoxy)-[3,4′-bipyridin]-2′(1′H)-one (**8c**).* Yellow solid; m.p. 178.1–179.2 °C; Yield: 71%. HPLC: 100%, t_R = 4.507 min ^{1}H NMR (500 MHz, DMSO-d_6) δ 11.40 (s, 1H), 7.88 (s, 1H), 7.55 (d, J = 8.2 Hz, 2H), 7.40 (d, J = 8.2 Hz, 2H), 7.33 (d, J = 6.8 Hz, 1H), 7.26 (s, 1H), 6.47-6.38 (m, 2H), 6.28 (s, 2H), 5.84-5.74 (m, 1H), 2.32 (s, 3H), 1.57 (d, J = 6.3 Hz, 3H). ^{13}C NMR (500 MHz, DMSO-d_6) δ 162.7, 152.6, 149.6, 139.6139.2, 137.4, 136.8, 135.1, 129.0, 125.8, 120.6, 115.5, 113.2, 102.9, 74.6, 23.9, 20.7. HRMS (ESI) *m/z* calcd for $C_{19}H_{20}N_3O_2$ $[M+H]^+$: 322.1550, Found: 322.1552.

*4.1.6.4. 6-Amino-1′-methyl-5-(1-(p-tolyl) ethoxy)-[3,4′-bipyridin]-2′(1′H)-one (**8d**).* Yellow solid; m.p. 186–187 °C; Yield: 76%. HPLC: 95.89%, t_R = 4.620 min ^{1}H NMR (500 MHz, $CDCl_3$) δ 7.84 (s, 1H), 7.24 (t, J = 7.1 Hz, 3H), 7.16 (d, J = 7.9 Hz, 2H), 6.95 (d, J = 1.3 Hz, 1H), 6.52 (d, J = 1.5 Hz, 1H), 6.24 (d, J = 7.0 Hz, 1H), 5.33 (q, J = 6.4 Hz, 1H), 5.26 (s, 2H), 3.52 (s, 3H), 2.32 (s, 3H), 1.67 (d, J = 6.4 Hz, 3H). ^{13}C NMR (500 MHz, DMSO-d_6) δ 162.1, 152.6, 148.6, 139.6, 139.3, 139.3, 137.4, 136.8, 129.0, 125.8, 120.3, 115.5, 112.2, 103.0, 74.7, 36.2, 23.8, 20.7. HRMS (ESI) *m/z* calcd for $C_{20}H_{22}N_3O_2$ $[M+H]^+$: 336.1707, Found: 336.1702.

*4.1.6.5. 6-Amino-5-(1-(4-chlorophenyl) ethoxy)-[3, 4′-bipyridin]-2′(1′H)-one (**8e**).* Black solid; m.p. 189–192 °C; Yield: 62%. HPLC: 100%, t_R = 4.693 min ^{1}H NMR (500 MHz, DMSO-d_6) δ 11.41 (s, 1H), 7.89 (s, 1H), 7.54 (d, J = 8.3 Hz, 2H), 7.41 (d, J = 8.3 Hz, 2H), 7.33 (d, J = 6.8 Hz, 1H), 7.26 (s, 1H), 6.47-6.38 (m, 2H), 6.28 (s, 2H), 5.84-5.74 (m, 1H), 1.57 (d, J = 6.3 Hz, 3H). ^{13}C NMR (500 MHz, DMSO-d_6) δ162.7, 152.6, 149.5, 141.7, 139.0, 137.7, 135.1, 132.1, 128.5, 127.9, 120.6, 115.6, 113.2, 102.9, 74.0, 23.6. HRMS (ESI) *m/z* calcd for $C_{18}H_{17}ClN_3O_2$ $[M+H]^+$: 342.1004, Found: 342.1001.

*4.1.6.6. 6-Amino-5-(1-(4-chlorophenyl) ethoxy)-1′-methyl-[3, 4′-bipyridin]-2′(1′H)-one (**8f**).* Grey solid; m.p. 257–259 °C; Yield: 67%. HPLC: 100%, t_R = 4.807 min.^{1}H NMR (500 MHz, $CDCl_3$) δ 7.85 (d, J = 1.1 Hz, 1H), 7.33 (dd, J = 20.9, 8.5 Hz, 4H), 7.27 (d, J = 7.1 Hz, 1H), 6.92 (d, J = 1.3 Hz, 1H), 6.55 (d, J = 1.5 Hz, 1H), 6.26 (dd, J = 7.0, 1.7 Hz, 1H), 5.36 (dd, J = 12.6, 6.1 Hz, 3H), 3.55 (s, 3H), 1.69 (d, J = 6.4 Hz, 3H). ^{13}C NMR (500 MHz, DMSO-d_6) δ 162.1, 152.5, 148.4, 141.6, 139.3, 139.0, 137.5, 132.1, 128.4, 127.9, 120.2, 115.6, 112.2, 102.9, 74.0, 36.2, 23.5. HRMS (ESI) *m/z* calcd for $C_{19}H_{19}ClN_3O_2$ $[M+H]^+$: 356.1160, Found: 356.1157.

*4.1.6.7. 6-Amino-5-(1-(2, 6-dichloro-3-fluorophenyl)ethoxy)-[3,4′-bipyridin]-2′(1′H)-one (**8g**).* Yellow solid; m.p. 250–252 °C; Yield: 71%. HPLC: 99.58%, t_R = 5.027 min ^{1}H NMR (500 MHz, DMSO-d_6) δ 11.43 (s, 1H), 7.92 (d, J = 1.8 Hz, 1H), 7.57 (dd, J = 9.0, 4.9 Hz, 1H), 7.46 (t, J = 8.7 Hz, 1H), 7.34 (d, J = 6.9 Hz, 1H), 6.94 (d, J = 1.6 Hz, 1H), 6.32 (dd, J = 6.9, 1.7 Hz, 1H), 6.27 (d, J = 1.5 Hz, 1H), 6.21 (s, 2H), 6.16 (t, J = 6.6 Hz, 1H), 1.81 (d, J = 6.6 Hz, 3H). ^{13}C NMR (500 MHz, DMSO-d_6) δ 162.6, 156.8 (d, J = 246.3 Hz), 152.1, 149.3, 138.5, 138.1, 136.7, 135.3, 130.6 (d, J = 5.0 Hz), 128.7 (d, J = 2.5 Hz), 121.0 (d, J = 18.8 Hz), 120.5117.5 (d, J = 23.8 Hz), 114.2, 113.1, 102.6 72.1, 18.7. HRMS (ESI) *m/z* calcd for $C_{18}H_{15}Cl_2FN_3O_2$ $[M+H]^+$: 394.0520, Found: 394.0516.

*4.1.6.8. 6-Amino-5-(1-(2, 6-dichloro-3-fluorophenyl) ethoxy)-1′-methyl-[3, 4′-bipyridin]-2′(1′H)-one (**8h**).* Yellow solid; m.p. 130–133 °C; Yield: 78%. HPLC: 95.73%, t_R = 5.193 min ^{1}H NMR (500 MHz, $CDCl_3$) δ 7.92 (d, J = 1.7 Hz, 1H), 7.35 (dd, J = 8.9, 4.8 Hz, 1H), 7.09 (dd, J = 8.8, 8.0 Hz, 1H), 6.99 (d, J = 1.8 Hz, 1H), 6.60 (d, J = 2.0 Hz, 1H), 6.27 (dd, J = 7.1, 2.1 Hz, 1H), 6.13 (q, J = 6.7 Hz, 1H), 5.07 (d, J = 23.9 Hz, 2H), 3.56 (s, 3H), 1.88 (d, J = 6.7 Hz, 3H). ^{13}C NMR (500 MHz, DMSO-d_6) δ 161.9, 156.8 (d, J = 245.0 Hz), 152.1, 148.3, 139.6, 138.5, 138.1, 136.7, 130.6 (d, J = 8.8 Hz), 128.7 (d, J = 3.8 Hz), 121.0 (d, J = 18.8 Hz), 120.2, 117.5 (d, J = 23.8 Hz), 114.1,

112.1, 102.6, 72.1, 36.2, 18.7. HRMS (ESI) *m/z* calcd for $C_{19}H_{17}Cl_2FN_3O_2$ $[M+H]^+$: 408.0676, Found: 408.0672.

*4.1.6.9. 6-Amino-1′-methyl-5-(1-(pyridin-2-yl) ethoxy)-[3, 4′-bipyridin]-2′(1′H)-one (**8i**).* Black solid; m.p. 204–207 °C; Yield: 46%. HPLC: 100%, $t_R = 3.360$ min ^{1}H NMR (500 MHz, DMSO-d_6) δ 8.53 (d, $J = 4.2$ Hz, 1H), 7.89 (d, $J = 1.8$ Hz, 1H), 7.78 (td, $J = 7.7$, 1.6 Hz, 1H), 7.62 (d, $J = 7.0$ Hz, 1H), 7.53 (d, $J = 7.9$ Hz, 1H), 7.28 (dd, $J = 6.6$, 4.9 Hz, 1H), 7.20 (d, $J = 1.7$ Hz, 1H), 6.49–6.35 (m, 2H), 6.27 (s, 2H), 5.68 (q, $J = 6.4$ Hz, 1H), 3.37 (s, 3H), 1.61 (d, $J = 6.4$ Hz, 3H). ^{13}C NMR (500 MHz, DMSO-d_6) δ 162.0, 161.3, 152.5, 148.9, 148.5, 139.4, 139.2, 137.7, 137.2, 122.9, 120.3, 120.0, 115.5, 112.2, 102.9, 76.3, 36.2, 21.8. HRMS (ESI) *m/z* calcd for $C_{18}H_{19}N_4O_2$ $[M+H]^+$: 323.1503, Found: 323.1507.

*4.1.6.10. 6-Amino-1′-methyl-5-(1-(pyridin-3-yl) ethoxy)-[3, 4′-bipyridin]-2′(1′H)-one (**8j**).* Black solid; m.p. 203–205 °C; Yield: 41%. HPLC: 100%, $t_R = 2.567$ min ^{1}H NMR (500 MHz, DMSO-d_6) δ 8.72 (s, 1H), 8.54-8.38 (m, 1H), 7.92 (ddd, $J = 8.6$, 5.2, 1.9 Hz, 2H), 7.63 (d, $J = 7.1$ Hz, 1H), 7.42-7.32 (m, 2H), 6.54 (d, $J = 2.0$ Hz, 1H), 6.48 (dd, $J = 7.2$, 2.1 Hz, 1H), 6.31 (s, 2H), 5.86 (q, $J = 6.3$ Hz, 1H), 3.39 (d, $J = 10.3$ Hz, 3H), 1.59 (d, $J = 6.4$ Hz, 3H). ^{13}C NMR (500 MHz, DMSO-d_6) δ 162.1, 152.7, 148.9, 148.4, 147.8, 139.3, 138.8, 137.8, 133.7, 123.7, 120.2, 115.8, 112.2, 102.9, 72.8, 36.2, 23.2. HRMS (ESI) *m/z* calcd for $C_{18}H_{19}N_4O_2$ $[M+H]^+$: 323.1503, Found: 323.1510.

*4.1.6.11. 6-Amino-1′-methyl-5-(1-(pyridin-4-yl) ethoxy)-[3, 4′-bipyridin]-2′(1′H)-one (**8k**).* Yellow oil; Yield: 38%. HPLC: 100%, $t_R = 2.287$ min.^{1}H NMR (500 MHz, $CDCl_3$) δ 8.61 (d, $J = 5.8$ Hz, 2H), 7.91 (d, $J = 1.6$ Hz, 1H), 7.28 (d, $J = 5.9$ Hz, 2H), 7.25 (d, $J = 7.2$ Hz, 1H), 6.85 (d, $J = 1.5$ Hz, 1H), 6.52 (d, $J = 1.7$ Hz, 1H), 6.22 (dd, $J = 7.1$, 1.9 Hz, 1H), 5.36 (q, $J = 6.4$ Hz, 1H), 5.09 (s, 2H), 3.53 (s, 3H), 1.71 (d, $J = 6.5$ Hz, 3H). ^{13}C NMR (500 MHz, DMSO-d_6) δ 162.1, 152.4, 151.6, 151.4, 149.7, 139.4, 139.0, 121.0, 120.2, 115.6, 112.4, 102.9, 73.5, 36.2, 22.9. HRMS (ESI): *m/z* calcd for $C_{18}H_{19}N_4O_2$ $[M+H]^+$: 323.1503, Found: 323.1500.

*4.1.6.12. 6-Amino-1′-benzyl-5-(1-(2, 6-dichloro-3-fluorophenyl) ethoxy)-[3,4′-bipyridin]-2′(1′H)-one (**8l**).* Yellow solid; m.p. 89–91 °C; Yield: 62%. HPLC: 96.62%, $t_R = 6.160$ min ^{1}H NMR (500 MHz, $CDCl_3$) δ 7.93 (d, $J = 1.8$ Hz, 1H), 7.36 (tt, $J = 8.5$, 6.0 Hz, 6H), 7.27 (d, $J = 7.2$ Hz, 1H), 7.09 (dd, $J = 8.8$, 8.0 Hz, 1H), 6.99 (d, $J = 1.8$ Hz, 1H), 6.64 (d, $J = 2.0$ Hz, 1H), 6.28 (dd, $J = 7.2$, 2.1 Hz, 1H), 6.13 (q, $J = 6.7$ Hz, 1H), 5.17 (s, 2H), 5.06 (s, 2H), 1.88 (d, $J = 6.7$ Hz, 3H). ^{13}C NMR (500 MHz, DMSO-d_6) δ 161.5, 156.8 (d, $J = 245$ Hz), 152.3, 148.4, 138.9, 138.5, 138.3, 137.5, 136.6, 130.5, 128.7 (d, $J = 3.75$ Hz), 128.5, 127.8, 127.5, 121.0 (d, $J = 20$ Hz), 120.0, 117.5 (d, $J = 22.5$ Hz), 114.0, 112.6, 103.2, 72.1, 50.7, 18.6. HRMS (ESI) *m/z* calcd for $C_{25}H_{21}Cl_2FN_3O_2$ $[M+H]^+$: 484.0989, Found: 484.0992.

*4.1.7. General procedure for the synthesis of 2-amino-5-bromo-N-(1-(2,6-dichloro-3-fluorophenyl)ethyl)nicotinamide (**12**)*

To an ice-cold solution of 2-amino-5-bromonicotinic acid (0.6 mmol) in anhydrous DMF (5 mL), HATU (0.66 mmol), DIPEA (0.72 mmol) and 1-(2,6-dichloro-3-fluorophenyl)ethan-1-amine (0.72 mmol) was added portion-wise. The reaction mixture was warmed to room temperature and stirred at rt for 6 h. After the completion of the reaction, 20 mL of H_2O was added and the reaction mixture was extracted with EtOAc for 3 times. The combined organic layer was collected and rinsed with brine. The mixture was evaporated to obtain the crude product and purified by silica gel for **12**. Yield: 84%. ^{1}H NMR (500 MHz, $CDCl_3$) δ 8.17 (d, $J = 2.5$ Hz, 1H), 7.71 (d, $J = 2.5$ Hz, 1H), 7.29 (s, 1H), 7.07- 6.97 (m, 2H), 6.33 (s, 2H), 6.10-6.00 (m, 1H), 1.67 (d, $J = 7.5$ Hz, 3H). HRMS (ESI) *m/z* calcd for $C_{14}H_{12}BrCl_2FN_3O$, $[M+H]^+$: 405.9519, Found: 405.9519.

*4.1.8. General procedure for the synthesis of **13***

According to the synthetic procedure of **4.1.6**.

*4.1.8.1. 6-Amino-N-(1-(2, 6-dichloro-3-fluorophenyl) ethyl)-2′-oxo-1′, 2′-dihydro-[3, 4′-bipyridine]-5-carboxamide (**13a**).* Brown solid; m.p. 288–290 °C; Yield: 69%. HPLC: 95.62%, $t_R = 5.960$ min ^{1}H NMR (500 MHz, DMSO-d_6) δ 11.52 (s, 1H), 9.23 (d, $J = 5.0$ Hz, 1H), 8.48 (s, 1H), 8.40 (d, $J = 13.0$ Hz, 1H), 7.50–7.45 (m, 1H), 7.42 (d, $J = 6.8$ Hz, 1H), 7.34 (dd, $J = 17.3$, 8.6 Hz, 3H), 6.75 (s, 1H), 6.59 (d, $J = 6.5$ Hz, 1H), 5.69-5.54 (m, 1H), 1.60 (d, $J = 7.3$ Hz, 3H). ^{13}C NMR (500 MHz, DMSO-d_6) δ 171.0, 166.5, 162.8, 159.3, 156.6 (d, $J = 242.5$ Hz), 149.9, 148.8, 140.1, 135.5, 135.1, 119.9, 116.0, 115.8, 113.7, 108.3, 102.9, 47.6, 17.0. HRMS (ESI) *m/z* calcd for $C_{19}H_{16}Cl_2FN_4O_2$ $[M+H]^+$: 421.0629, Found: 421.0627.

*4.1.8.2. 6-Amino-N-(1-(2, 6-dichloro-3-fluorophenyl) ethyl)-1′-methyl-2′-oxo-1′, 2′-dihydro-[3, 4′-bipyridine]-5-carboxamide (**13b**).* Yellow solid; m. p. 290–293 °C; HPLC: 96.50%, $t_R = 6.087$ min ^{1}H NMR (500 MHz, DMSO-d_6) δ 9.22 (d, $J = 5.0$ Hz, 1H), 8.51 (s, 1H), 8.41 (s, 1H), 7.76 (d, $J = 7.0$ Hz, 1H), 7.48-7.46 (m, 1H), 7.37-7.34 (m, 3H), 6.86 (s, 1H), 6.67 (d, $J = 7.0$ Hz, 1H), 5.68-5.58 (m, 1H), 3.44 (s, 3H), 1.62 (d, $J = 7.5$ Hz, 3H). ^{13}C NMR (125 MHz, DMSO-d_6) δ 170.3, 166.4, 162.2, 159.3, 156.6 (d, $J = 244$ Hz), 149.8, 147.7, 140.1, 139.7, 135.0, 130.1 (d, $J = 8.8$ Hz), 119.5, 115.8 (d, $J = 23.8$ Hz), 112.6, 108.2, 102.8, 59.7, 36.3, 17.1. HRMS (ESI) *m/z* calcd for $C_{20}H_{18}Cl_2FN_4O_2$ $[M+H]^+$: 435.0785, Found: 435.0783.

*4.1.9. General procedure for the synthesis of (R)-3-(1-(2,6-dichloro-3-fluorophenyl) ethoxy)-2-nitropyridine (**15**)*

(*S*)-1-(2,6-dichloro-3-fluorophenyl) ethanol (20 mmol), PPh_3 (30 mmol) and 2-nitro-3-hydroxyl pyridine (20 mmol) were dissolved in 30 mL THF under the N_2 atmosphere. When the reaction was cooled to 0 °C, the DEAD (30 mmol) was added dropwise. Then the reaction was warmed to room temperature for 3 h. The reaction mixture was evaporated and crystallized by EtOH-Pet. Light yellow solid. Yield: 88%. ^{1}H NMR (500 MHz, $CDCl_3$) δ 8.01 (dd, $J = 4.5$, 1.5 Hz, 1H), 7.38-7.35 (m, 1H), 7.31-7.28 (m, 1H), 7.21 (dd, $J = 8.5$, 1.0 Hz, 1H), 7.07 (dd, $J = 9.0$, 8.0 Hz, 1H), 6.09 (q, $J = 7.0$ Hz, 1H), 1.83 (d, $J = 6.5$ Hz, 3H). HRMS (ESI) *m/z* calcd for $C_{13}H_{10}Cl_2FN_2O_3$ $[M+H]^+$: 331.0047, Found: 331.0046.

*4.1.10. General procedure for the synthesis of (R)-3-(1-(2,6-dichloro-3-fluorophenyl) ethoxy) pyridin-2-amine (**16**)*

The **15** (16 mmol) and Fe (48 mmol) were dissolved in 100 mL EtOH and 25 mL AcOH. The reaction was refluxed for 2 h. After the completion of reaction, the pH was adjusted to basic condition with Na_2CO_3 solution. The mixture was extracted with EtOAc and the combined organic layer was evaporated to get the crude product. The final product was crystallized with EtOAc/Pet [23]. Yield: 91%. HRMS (ESI) *m/z* calcd for $C_{13}H_{12}Cl_2FN_2O$ $[M+H]^+$: 301.0305, Found: 301.0306.

*4.1.11. General procedure for the synthesis of (R)-5-bromo-3-(1-(2,6-dichloro-3-fluorophenyl) ethoxy) pyridin-2-amine (**17**)*

The **16** (15 mmol) was dissolved in 50 mL MeCN and 25 mL CH_2Cl_2, NBS (15 mmol) was added to the above mixture portion-wise at ice-bath. After the reaction was stirred for 15 min, 5 mL H_2O was added to quench the reaction. The mixture was extracted with DCM and the combined organic layer was evaporated to get the crude product. The final product was crystallized with MeOH. Yield: 81%. ^{1}H NMR (500 MHz, $CDCl_3$) δ 7.66 (d, $J = 2.0$ Hz, 1H), 7.32-7.29 (m, 1H), 7.07 (dd, $J = 8.5$, 8.0 Hz, 1H), 6.83 (d, $J = 2.0$ Hz, 1H), 5.98 (q, $J = 7.0$ Hz, 1H), 4.85 (s, 2H), 1.81 (d, $J = 7.0$ Hz, 3H). HRMS (ESI) *m/z* calcd for $C_{13}H_{11}BrCl_2FN_2O$ $[M+H]^+$: 378.9410, Found: 378.9400.

*4.1.12. General procedure for the synthesis of **18***

According to the synthetic procedure of **4.1.6**.

*4.1.12.1. (R)-6-Amino-5-(1-(2,6-dichloro-3-fluorophenyl)ethoxy)-[3,4′-bipyridin]-2′(1′H)-one (**18a**).* Yellow solid; m.p. 265–267 °C; Yield: 69%. [α]25D = + 10 (c = 0.5, MeOH); HPLC: 97.39%, t_R = 5.020 min ^{1}H NMR (500 MHz, DMSO-d_6) δ 11.44 (s, 1H), 7.92 (s, 1H), 7.57 (dd, *J* = 8.9, 4.9 Hz, 1H), 7.45 (t, *J* = 8.7 Hz, 1H), 7.35 (d, *J* = 6.9 Hz, 1H), 6.94 (s, 1H), 6.35-6.30 (m, 1H), 6.28 (s, 1H), 6.22 (s, 2H), 6.15 (q, *J* = 6.5 Hz, 1H), 1.81 (d, *J* = 6.6 Hz, 3H). ^{13}C NMR (500 MHz, DMSO-d_6) δ 162.6, 156.8 (d, *J* = 246.3 Hz), 152.2, 149.4, 138.5, 138.1, 136.7, 135.3, 130.6, 128.7 (d, *J* = 3.8 Hz), 121.0 (d, *J* = 20.0 Hz), 120.5, 117.5 (d, *J* = 23.8 Hz), 114.2, 113.1, 102.7, 72.1, 18.7. HRMS (ESI) *m/z* calcd for $C_{18}H_{15}Cl_2FN_3O_2$ $[M+H]^+$: 394.0520, Found: 394.0527.

*4.1.12.2. (R)-6-Amino-5-(1-(2, 6-dichloro-3-fluorophenyl) ethoxy)-1′-methyl-[3, 4′-bipyridin]-2′(1′H)-one (**18b**).* Yellow solid; m.p. 109–111 °C; Yield: 75%. [α]25D = + 8 (c = 0.5, MeOH); HPLC: 95.83%, t_R = 5.160 min ^{1}H NMR (500 MHz, DMSO-d_6) δ 7.94 (s, 1H), 7.66 (d, *J* = 6.8 Hz, 1H), 7.57 (dd, *J* = 8.8, 4.8 Hz, 1H), 7.46 (t, *J* = 8.6 Hz, 1H), 6.95 (s, 1H), 6.37 (d, *J* = 6.5 Hz, 2H), 6.21 (s, 2H), 6.18-6.01 (m, 1H), 3.39 (s, 3H), 1.81 (d, *J* = 6.5 Hz, 3H). ^{13}C NMR (500 MHz, DMSO-d_6) δ 161.9, 156.8 (d, *J* = 246.3 Hz), 152.1, 148.3, 139.6, 138.5, 137.9, 136.6, 130.6, 128.7 (d, *J* = 2.5 Hz), 121.0 (d, *J* = 20.0 Hz), 120.2, 117.5 (d, *J* = 22.5 Hz), 114.2, 112.1, 102.6, 72.1, 36.2, 18.7. HRMS (ESI) *m/z* calcd for $C_{19}H_{17}Cl_2FN_3O_2$ $[M+H]^+$: 408.0676, Found: 408.0672.

*4.1.12.3. (R)-6-Amino-1′-benzyl-5-(1-(2, 6-dichloro-3-fluorophenyl) ethoxy)-[3,4′-bipyridin]-2′(1′H)-one (**18c**).* Yellow solid; m.p. 112–114 °C; Yield: 66%. [α]25D = + 43 (c = 0.5, MeOH); HPLC: 100%, t_R = 6.160 min ^{1}H NMR (500 MHz, DMSO-d_6) δ 7.96 (s, 1H), 7.77 (d, *J* = 7.1 Hz, 1H), 7.57 (dd, *J* = 8.9, 4.9 Hz, 1H), 7.45 (t, *J* = 8.7 Hz, 1H), 7.37-7.27 (m, 5H), 6.97 (s, 1H), 6.43 (d, *J* = 7.2 Hz, 1H), 6.40 (s, 1H), 6.25 (s, 2H), 6.16 (q, *J* = 6.5 Hz, 1H), 5.07 (s, 2H), 1.81 (d, *J* = 6.6 Hz, 3H). ^{13}C NMR (125 MHz, DMSO) δ 161.5, 156.8 (d, *J* = 245.0 Hz), 152.3, 148.4, 138.9, 138.5, 138.3, 137.5, 136.6, 130.5, 128.7, 128.5, 127.7, 127.5, 121.0 (d, *J* = 18.8 Hz), 120.0, 117.5 (d, *J* = 22.5 Hz), 114.1, 112.6, 103.2, 72.1, 50.7, 18.6. HRMS (ESI) *m/z* calcd for $C_{25}H_{21}Cl_2FN_3O_2$ $[M+H]^+$: 484.0989, Found: 484.0987.

*4.1.12.4. (R)-6-Amino-5-(1-(2, 6-dichloro-3-fluorophenyl) ethoxy)-1′-(2-(dimethylamino)ethyl)-[3,4′-bipyridin]-2′(1′H)-one (**18d**).* Yellow solid; m.p. 198–201 °C; Yield: 53%. [α]25D = + 27 (c = 0.5, MeOH); HPLC: 95.78%, t_R = 4.127 min ^{1}H NMR (500 MHz, DMSO-d_6) δ 7.95 (s, 1H), 7.65-7.54 (m, 2H), 7.45 (t, *J* = 8.6 Hz, 1H), 6.95 (s, 1H), 6.37 (dd, *J* = 23.1, 16.1 Hz, 2H), 6.22 (s, 2H), 6.15 (dd, *J* = 12.9, 6.3 Hz, 1H), 3.93 (t, *J* = 5.9 Hz, 2H), 2.49 (d, *J* = 6.1 Hz, 2H), 2.18 (s, 6H), 1.81 (d, *J* = 6.5 Hz, 3H). ^{13}C NMR (500 MHz, DMSO-d_6) δ 161.5, 156.8 (d, *J* = 245.0 Hz), 152.2, 148.2, 139.3, 138.5, 138.1, 130.6, 1128.7 (d, *J* = 2.5 Hz), 121.0 (d, *J* = 18.8 Hz), 120.1, 117.5 (d, *J* = 23.8 Hz), 114.1, 112.3, 102.5, 72.1, 57.5, 45.7, 45.3, 18.7. HRMS (ESI) *m/z* calcd for $C_{22}H_{24}Cl_2FN_4O_2$ $[M+H]^+$: 465.1255, Found:465.1258.

*4.1.12.5. (R)-6-Amino-5-(1-(2, 6-dichloro-3-fluorophenyl) ethoxy)-1′-propyl-[3, 4′-bipyridin]-2′(1′H)-one (**18e**).* White solid; m.p. 184–186 °C; Yield: 68%. [α]25D = + 13 (c = 0.5, MeOH); HPLC: 96.96%, t_R = 5.447 min ^{1}H NMR (500 MHz, DMSO-d_6) δ 7.91 (d, *J* = 1.9 Hz, 1H), 7.69-7.62 (m, 1H), 7.55 (dd, *J* = 9.0, 4.9 Hz, 1H), 7.44 (t, *J* = 8.7 Hz, 1H), 6.92 (d, *J* = 1.9 Hz, 1H), 6.36 (dd, *J* = 7.2, 2.1 Hz, 1H), 6.32 (d, *J* = 2.0 Hz, 1H), 6.21 (s, 2H), 6.13 (q, *J* = 6.6 Hz, 1H), 3.85 (q, *J* = 7.1 Hz, 2H), 1.18 (t, *J* = 7.1 Hz, 3H). ^{13}C NMR (500 MHz, DMSO-d_6) δ 161.3, 156.8 (d, *J* = 245.0 Hz), 152.2, 148.2, 138.5, 138.1, 136.7, 130.6, 128.7 (d, *J* = 3.8 Hz), 121.0 (d, *J* = 18.8 Hz), 120.1, 117.5 (d, *J* = 22.5 Hz), 114.1, 112.4, 102.9, 72.1, 43.1, 18.7, 14.5. HRMS (ESI) *m/z* calcd for $C_{20}H_{19}Cl_2FN_3O_2$ $[M+H]^+$: 422.0833, Found: 422.0831.

*4.1.12.6. Ethyl (R)-2-(6-amino-5-(1-(2, 6-dichloro-3-fluorophenyl) ethoxy)-2′-oxo-[3, 4′-bipyridin]-1′(2′H)-yl)acetate (**18f**).* Yellow solid; m.p. 142–145 °C; Yield: 57%. [α]25D = + 34 (c = 0.5, MeOH); HPLC: 96.82%, t_R = 5.467 min ^{1}H NMR (500 MHz, DMSO-d_6) δ 7.95 (d, *J* = 1.7 Hz, 1H), 7.63 (d, *J* = 7.2 Hz, 1H), 7.55 (dd, *J* = 8.9, 4.9 Hz, 1H), 7.43 (t, *J* = 8.7 Hz, 1H), 6.94 (d, *J* = 1.5 Hz, 1H), 6.43 (dd, *J* = 7.2, 1.9 Hz, 1H), 6.36 (d, *J* = 1.8 Hz, 1H), 6.26 (s, 2H), 6.14 (q, *J* = 6.6 Hz, 1H), 4.63 (s, 2H), 4.12 (q, *J* = 7.1 Hz, 2H), 1.79 (d, *J* = 6.6 Hz, 3H), 1.19 (t, *J* = 7.1 Hz, 3H). ^{13}C NMR (500 MHz, DMSO-d_6) δ168.2, 161.5, 156.9 (d, *J* = 243.8 Hz), 152.3, 149.1, 139.4, 138.5, 138.4, 136.7, 130.6, 128.7 (d, *J* = 3.8 Hz), 121.0 (d, *J* = 18.8 Hz), 119.9, 117.6 (d, *J* = 22.5 Hz), 114.1, 112.0, 103.0, 72.1, 61.0, 49.7, 18.7, 14.1. HRMS (ESI): *m/z* calcd for $C_{22}H_{21}Cl_2FN_3O_4$ $[M+H]^+$: 480.0888, Found: 480.0882.

*4.1.12.7. (R)-6-Amino-5-(1-(2, 6-dichloro-3-fluorophenyl) ethoxy)-1′-propyl-[3, 4′-bipyridin]-2′(1′H)-one (**18g**).* Yellow solid; m.p. 157–159 °C; Yield: 65%. [α]25D = + 16 (c = 0.5, MeOH); HPLC: 95.72%, t_R = 5.820 min.^{1}H NMR (500 MHz, DMSO-d_6) δ 7.92 (d, *J* = 1.8 Hz, 1H), 7.62 (d, *J* = 7.1 Hz, 1H), 7.54 (dd, *J* = 8.9, 4.9 Hz, 1H), 7.42 (t, *J* = 8.7 Hz, 1H), 6.92 (d, *J* = 1.8 Hz, 1H), 6.38-6.30 (m, 2H), 6.21 (s, 2H), 6.12 (q, *J* = 6.6 Hz, 1H), 3.81-3.70 (m, 2H), 1.78 (d, *J* = 6.6 Hz, 3H), 1.61 (dt, *J* = 14.6, 7.3 Hz, 2H), 0.83 (t, *J* = 7.4 Hz, 3H). ^{13}C NMR (500 MHz, DMSO-d_6) δ 161.5, 156.8 (d, *J* = 246.3 Hz), 152.2, 148.1, 139.0, 138.5, 138.1, 136.7, 130.6, 128.7 (d, *J* = 3.8 Hz), 121.0 (d, *J* = 18.8 Hz), 120.1, 117.5 (d, *J* = 22.5 Hz), 114.1, 112.4, 102.7, 72.1, 49.6, 22.0, 18.7, 10.9. HRMS (ESI) *m/z* calcd for $C_{21}H_{21}Cl_2FN_3O_2$ $[M+H]^+$: 436.0989 Found: 436.0989.

*4.1.13. General procedure for the synthesis of (R)-5-bromo-3-((1-(2,6-dichloro-3-fluorophenyl) ethyl) thio) pyridin-2-amine (**24**)*

The general synthesis was according to the literature [25]. Yield: 58%. ^{1}H NMR (500 MHz, $CDCl_3$) δ 8.03 (t, *J* = 3.0 Hz, 1H), 7.51 (dd, *J* = 9.5, 2.5 Hz, 1H), 7.29 (dd, *J* = 9.0, 5.0 Hz, 0.5H), 7.20 (dd, *J* = 9.0, 5.0 Hz, 0.5H), 7.01 (t, *J* = 8.0 Hz, 1H), 5.17 (s, 2H), 5.05-4.97 (m, 1H), 1.82 (dd, *J* = 7.5, 4.5Hz, 3H).

*4.1.14. General procedure for the synthesis of **25***

The general synthesis was according to the procedure for **4.1.6**.

*4.1.14.1. (R)-6-Amino-5-((1-(2, 6-dichloro-3-fluorophenyl) ethyl) thio)-[3, 4′-bipyridin]-2′(1′H)-one (**25a**).* Yellow solid; m.p. 230–233 °C; Yield: 75%. [α]25D = + 134 (c = 0.25, MeOH); HPLC: 100%, t_R = 6.220 min ^{1}H NMR (500 MHz, DMSO-d_6) δ 11.44 (s, 1H), 8.32 (s, 1H), 7.46 (dd, *J* = 17.6, 2.0 Hz, 1H), 7.38-7.32 (m, 2H), 6.64 (d, *J* = 5.0 Hz, 2H), 6.39 -6.14 (m, 2H), 5.07 (d, *J* = 7.2 Hz, 1H), 2.09-1.64 (m, 3H). ^{13}C NMR (500 MHz, DMSO-d_6) δ162.6, 161.0, 160.9, 157.2(d, *J* = 243.8 Hz), 155.9 (d, *J* = 245.0 Hz), 148.5, 147.9, 147.8, 142.1, 142.0, 139.1, 139.0, 135.4, 131.1, 131.0, 129.6 (d, *J* = 2.5 Hz), 129.2 (d, *J* = 2.5 Hz), 129.1, 129.0, 121.9, 121.8, 121.5 (d, *J* = 17.5 Hz), 121.3, 116.3 (d, *J* = 23.8 Hz), 116.2 (d, *J* = 22.5 Hz), 113.2, 110.4, 110.3, 102.6, 43.9, 43.1, 18.3, 18.2. HRMS (ESI) *m/z* calcd for $C_{18}H_{15}Cl_2FN_3OS$ $[M+H]^+$: 410.0291, Found: 410.0296.

*4.1.14.2. (R)-6-Amino-5-((1-(2, 6-dichloro-3-fluorophenyl) ethyl) thio)-1′-methyl-[3,4′-bipyridin]-2′(1′H)-one (**25b**).* Yellow solid; m.p. 194–197 °C; Yield: 77%. [α]25D = + 134 (c = 0.5, MeOH); HPLC: 95.81%, t_R = 6.327 min ^{1}H NMR (500 MHz, DMSO-d_6) δ 8.34 (dd, *J* = 3.6, 2.5 Hz, 1H), 7.67 (d, *J* = 7.1 Hz, 1H), 7.50 (dd, *J* = 15.7, 2.4 Hz, 1H), 7.36 (dt, *J* = 9.6, 2.9 Hz, 1H), 6.65 (s, 2H), 6.37 (ddd, *J* = 8.3, 7.3, 1.6 Hz, 2H), 5.12-5.01 (m, 1H), 3.40 (d, *J* = 0.9 Hz, 3H), 1.81 (dd, *J* = 7.4, 1.9 Hz, 3H). ^{13}C NMR (500 MHz, DMSO-d_6) δ 161.9, 161.0, 160.9, 157.1 (d, *J* = 245.0 Hz), 155.9 (d, *J* = 245.0 Hz), 147.8, 147.7, 147.4, 142.0, 141.9. 139.7, 139.6, 139.2, 139.1, 131.0, 130.9, 129.6,

129.2 (d, $J = 3.8$ Hz), 129.1, 129.0, 121.0, 120.9, 116.3 (d, $J = 23.8$ Hz), 116.2 (d, $J = 22.5$ Hz), 112.1, 110.4, 102.5, 43.9, 43.2, 36.2, 18.3, 18.2. HRMS (ESI) *m/z* calcd for $C_{19}H_{17}Cl_2FN_3OS$ $[M+H]^+$: 424.0448, Found: 424.0446.

*4.1.14.3. (R)-6-Amino-1′-benzyl-5-((1-(2, 6-dichloro-3-fluorophenyl) ethyl)thio)-[3,4′-bipyridin]-2′(1′H)-one (**25c**).* Yellow solid; m.p. 64–68 °C; Yield: 67%. [α]25D = + 93 (c = 0.25, MeOH); HPLC: 95.25%, $t_R = 6.967$ min ^{1}H NMR (500 MHz, $CDCl_3$) δ 8.28 (t, $J = 2.2$ Hz, 1H), 7.64 (d, $J = 2.3$ Hz, 1H), 7.38-7.30 (m, 6H), 7.02 (dd, $J = 8.8$, 8.0 Hz, 1H), 6.63 (dd, $J = 9.3$, 1.9 Hz, 1H), 6.26 (td, $J = 7.1$, 2.1 Hz, 1H), 5.48 (d, $J = 5.0$ Hz, 2H), 5.17 (s, 2H), 5.06 (ddt, $J = 8.8$, 7.4, 4.4 Hz, 1H), 1.86 (dd, $J = 7.3$, 4.8 Hz, 3H). ^{13}C NMR (500 MHz, DMSO-d_6) δ 161.4, 161.1, 161.0, 157.2 (d, $J = 243.8$ Hz), 155.9 (d, $J = 245.0$ Hz), 148.0, 147.9, 147.6, 142.1, 142.0, 139.2, 139.1, 139.0, 137.5, 131.1, 131.0, 129.6 (d, $J = 3.8$ Hz), 129.2 (d, $J = 2.5$ Hz), 129.1, 129.0, 128.5, 127.7, 127.7, 127.5, 121.8 (d, $J = 20.0$ Hz), 121.5 (d, $J = 17.5$ Hz), 120.9, 120.8, 116.3 (d, $J = 22.5$ Hz), 116.2 (d, $J = 22.5$ Hz), 112.8, 110.5, 103.2, 50.7, 43.9, 43.2, 18.4, 18.3. HRMS (ESI) *m/z* calcd for $C_{25}H_{21}Cl_2FN_3OS$ $[M+H]^+$: 500.0761, Found: 500.0758.

*4.1.14.4. (R)-6-Amino-5-((1-(2, 6-dichloro-3-fluorophenyl) ethyl) thio)-1′-(2-(dimethylamino)ethyl)-[3,4′-bipyridin]-2′(1′H)-one (**25d**).* Brown solid; m.p. 192–195 °C; Yield: 61%. [α]25D = + 157 (c = 0.1, MeOH); HPLC: 96.29%, $t_R = 5.100$ min ^{1}H NMR (500 MHz, DMSO-d_6) δ 8.34 (dd, $J = 3.6$, 2.5 Hz, 1H), 7.61 (d, $J = 7.1$ Hz, 1H), 7.50 (dd, $J = 13.3$, 2.4 Hz, 1H), 7.43-7.23 (m, 2H), 6.63 (s, 2H), 6.40-6.28 (m, 2H), 5.12-5.01 (m, 1H), 3.95 (t, $J = 6.2$ Hz, 2H), 2.55- 2.51 (m, 2H), 2.20 (s, 6H), 1.81 (dd, $J = 7.4$, 2.3 Hz, 3H). ^{13}C NMR (500 MHz, DMSO-d_6) δ 161.6, 161.1, 161.0, 157.2 (d, $J = 245.0$ Hz), 155.9 (d, $J = 245.0$ Hz), 148.0, 147.9, 147.6, 142.1, 142.0, 139.4, 139.2, 139.1, 131.1, 131.0, 129.6 (d, $J = 3.8$ Hz), 129.2 (d, $J = 3.8$ Hz), 129.1, 129.0, 121.8 (d, $J = 18.8$ Hz), 121.5 (d, $J = 17.5$ Hz), 121.0, 120.9, 116.3 (d, $J = 22.5$ Hz), 116.2 (d, $J = 22.5$ Hz), 112.4, 110.5, 102.8, 56.9, 45.2, 44.6, 44.0, 43.2, 18.4, 18.3. HRMS (ESI) *m/z* calcd for $C_{22}H_{24}Cl_2FN_4OS$ $[M+H]^+$: 481.1026, Found: 481.1020.

4.2. Biological evaluation

4.2.1. Kinase inhibitory assay

The assays were performed *in vitro* using Homogeneous time resolved fluorescence (HTRF) method (Cisbio). ALK, ALK ^{L1196M}, ALK ^{G1202R} and ROS1 were purchased from Carna. The kinases and substrates were incubated first with synthesized analogues for 5 min in enzymatic buffer. Then ATP (Sigma) was added into the reaction mixture to start the enzyme reaction. The ATP concentrations used in each enzyme reaction were 24 μM (ALK) and 37 μM (ROS1), equivalent to the Km of ATP for the corresponding enzyme in this assay condition. The assays were conducted at room temperature for 30 min and stopped by detection reagents which contain EDTA. The detection step lasted for 1 h. The IC_{50} was calculated using GraphPad Prism 5.0.

4.2.2. Cell proliferation assay

All the cell lines were purchased from American type culture collection (ATCC). The cancer cells were seeded in density of 3500 cells/well, in 96-well plates (Corning) for 24 h. Duplicate wells were treated with test or reference compounds for 72 h at various concentrations or DMSO (Sigma) as control. Plates were incubated at 37 °C in 5% CO_2 atmosphere. Cell proliferation was determined by using MTT assay. The IC_{50} was calculated using GraphPad Prism 5.0.

4.2.3. Cell cycle analysis

Cells were treated with compounds at indicated concentration for 48 h, typsinized and fixed for 1 h at −20 °C by 70% ethanol. Then, the fixed cells were stained with propidium iodide (10 μg/mL) for 30 min at 37 °C and cell cycle variables analyzed by fluorescence-activated cell sorting analysis (BD).

4.3. Computational methods for molecular docking

The molecular modeling simulations were performed using Tripos Sybyl x1.3 molecular modeling package [42]. The co-crystal structure of ALK $^{[L1196M]}$ in complex with crizotinib was obtained from the RSC Protein Data Bank (http://www.rcsb.org) (PDB code: 2YFX). The initial structure of **18d** was generated by Sketch module in Sybyl x1.3. The geometries of the compound were subsequently optimized using the Tripos force field with Gasteiger-Hückel charges. The produced conformation of **18d** was then inserted into the binding pocket of ALK $^{[L1196M]}$ to replace ligand crizotinib for the initial structural model of **18d** binding to ALK $^{[L1196M]}$. Molecular docking studies of **18d** with the ALK $^{[L1196M]}$ binding pocket was performed with FlexiDock module in Sybyl x1.3 [43]. The docked complexes of inhibitor–enzyme were selected according to the criteria of interacting energy combined with geometrical matching quality. These complexes were used as the starting conformation for the geometrical optimization to achieve the final models of **18d** binding to ALK $^{[L1196M]}$. The ALK $^{[G1202R/L1196M]}$ model was built using 2YFX as a template.

Declaration of competing interest

The authors declare no conflict of interest.

Acknowledgments

We thank Marc A. Giulianotti in Torry Pines Institute for Molecular Studies, USA, for critical reading this manuscript. This project was supported by Zhejiang Provincial Natural Science Foundationof China (No. LY18H300001) to W. Chen; National Key R&D Program of China (No. 2017YFE0102200) and Osteoporosis & Breast Cancer Research Center, USA to Y. Yu. We thank Jianyang Pan (Research and Service Center, College of Pharmaceutical Sciences, Zhejiang University) for performing NMR spectrometry for structural elucidation.

Appendix A. Supplementary data

Supplementary data to this article can be found online at https://doi.org/10.1016/j.ejmech.2019.111734.

References

[1] M.A. Lemmon, J. Schlessinger, Cell signaling by receptor tyrosine kinases, Cell 141 (2010) 1117–1134.
[2] S.W. Morris, M.N. Kirstein, M.B. Valentine, K.G. Dittmer, D.N. Shapiro, D.L. Saltman, A.T. Look, Fusion of a kinase gene, ALK, to a nucleolar protein gene, NPM, in non-Hodgkin's lymphoma, Science 263 (1994) 1281–1284.
[3] M. Soda, Y.L. Choi, M. Enomoto, S. Takada, Y. Yamashita, S. Ishikawa, S. Fujiwara, H. Watanabe, K. Kurashina, H. Hatanaka, M. Bando, S. Ohno, Y. Ishikawa, H. Aburatani, T. Niki, Y. Sohara, Y. Sugiyama, H. Mano, Identification of the transforming EML4-ALK fusion gene in non-small-cell lung cancer, Nature 448 (2007) 561–566.
[4] Y.P. Mosse, M. Laudenslager, L. Longo, K.A. Cole, A. Wood, E.F. Attiyeh, M.J. Laquaglia, R. Sennett, J.E. Lynch, P. Perri, G. Laureys, F. Speleman, C. Kim, C. Hou, H. Hakonarson, A. Torkamani, N.J. Schork, G.M. Brodeur, G.P. Tonini, E. Rappaport, M. Devoto, J.M. Maris, Identification of ALK as a major familial neuroblastoma predisposition gene, Nature 455 (2008) 930–935.
[5] C.M. Coffin, A. Patel, S. Perkins, K.S. Elenitoba-Johnson, E. Perlman, C.A. Griffin, ALK1 and p80 expression and chromosomal rearrangements involving 2p23 in inflammatory myofibroblastic tumor, Mod. Pathol. 14 (2001) 569–576.
[6] K. Pulford, L. Lamant, S.W. Morris, L.H. Butler, K.M. Wood, G. Stroud, G. Delsol, D.Y. Mason, Detection of anaplastic lymphoma kinase (ALK) and nucleolar protein nucleophosmin (NPM)-ALK proteins in normal and neoplastic cells with the monoclonal antibody ALK1, Blood 89 (1997) 1394–1404.

[7] Y. Chen, J. Takita, Y.L. Choi, M. Kato, M. Ohira, M. Sanada, L. Wang, M. Soda, A. Kikuchi, T. Igarashi, A. Nakagawara, Y. Hayashi, H. Mano, S. Ogawa, Oncogenic mutations of ALK kinase in neuroblastoma, Nature 455 (2008) 971–974.

[8] M. Boi, E. Zucca, G. Inghirami, F. Bertoni, Advances in understanding the pathogenesis of systemic anaplastic large cell lymphomas, Br. J. Haematol. 168 (2015) 771–783.

[9] J. Duyster, R.Y. Bai, S.W. Morris, Translocation involving anaplastic lymphoma kinase (ALK), Oncogene 20 (2001) 5623–5637.

[10] L. Lamant, K. Pulford, D. Bischof, S.W. Morris, D.Y. Mason, G. Delsol, B. Mariamé, Expression of the ALK tyrosine kinase gene in neuroblastoma, Am. J. Pathol. 156 (2000) 1711–1721.

[11] B.M. Ku, J.-M. Sun, S.-h. Lee, J.S. Ahn, K. Park, M.-J. Ahn, An update on biomarkers for kinase inhibitor response in non-small-cell lung cancer, Expert Rev. Mol. Diagn 17 (2017) 933–942.

[12] C.M. Della Corte, G. Viscardi, R. Di Liello, M. Fasano, E. Martinelli, T. Troiani, F. Ciardiello, F. Morgillo, Role and targeting of anaplastic lymphoma kinase in cancer, Mol. Cancer 17 (2016) 30.

[13] D.R. Camidge, Y.J. Bang, E.L. Kwak, A.J. Iafrate, M. Varella-Garcia, S.B. Fox, G.J. Riely, B. Solomon, S.H. Ou, D.W. Kim, R. Salgia, P. Fidias, J.A. Engelman, L. Gandhi, P.A. Jänne, D.B. Costa, G.I. Shapiro, P. Lorusso, K. Ruffner, P. Stephenson, Y. Tang, K. Wilner, J.W. Clark, A.T. Shaw, Activity and safety of crizotinib in patients with ALK-positive non-small-cell lung cancer: updated results from a phase 1 study, Lancet Oncol. 13 (2012) 1011–1019.

[14] Y.P. Mosse, M.S. Lim, S.D. Voss, K. Wilner, K. Ruffner, J. Laliberte, D. Rolland, F.M. Balis, J.M. Maris, B.J. Weigel, A.M. Ingle, C. Ahern, P.C. Adamson, S.M. Blaney, Safety and activity of crizotinib for paediatric patients with refractory solid tumours or anaplastic large-cell lymphoma: a Children's oncology group phase I consortium study, Lancet Oncol. 14 (2013) 472–480.

[15] Y.L. Choi, M. Soda, Y. Yamashita, T. Ueno, J. Takashima, T. Nakajima, Y. Yatabe, K. Takeuchi, T. Hamada, H. Haruta, Y. Ishikawa, H. Kimura, T. Mitsudomi, Y. Tanio, H. Mano, ALK Lung Cancer Study Group. EML4-ALK mutations in lung cancer that confer resistance to ALK inhibitors, N. Engl. J. Med. 363 (2010) 1734–1739.

[16] T. Sasaki, K. Okuda, W. Zheng, J. Butrynski, M. Capelletti, L. Wang, N.S. Gray, K. Wilner, J.G. Christensen, G. Demetri, G.I. Shapiro, S.J. Rodig, M.J. Eck, P.A. Jänne, The neuroblastoma-associated F1174L ALK mutation causes resistance to an ALK kinase inhibitor in ALK-translocated cancers, Cancer Res. 70 (2010) 10038–10043.

[17] J.M. Heuckmann, M. Holzel, M.L. Sos, S. Heynck, H. Balke-Want, M. Koker, M. Peifer, J. Weiss, C.M. Lovly, C. Grütter, D. Rauh, W. Pao, R.K. Thomas, ALK mutations conferring differential resistance to structurally diverse ALK inhibitors, Clin. Cancer Res. 17 (2011) 7394–7401.

[18] T.H. Marsilje, W. Pei, B. Chen, W. Lu, T. Uno, Y. Jin, T. Jiang, S. Kim, N. Li, M. Warmuth, Y. Sarkisova, F. Sun, A. Steffy, A.C. Pferdekamper, A.G. Li, S.B. Joseph, Y. Kim, B. Liu, T. Tuntland, X. Cui, N.S. Gray, R. Steensma, Y. Wan, J. Jiang, G. Chopiuk, J. Li, W.P. Gordon, W. Richmond, K. Johnson, J. Chang, T. Groessl, Y.Q. He, A. Phimister, A. Aycinena, C.C. Lee, B. Bursulaya, D.S. Karanewsky, H.M. Seidel, J.L. Harris, P.Y. Michellys, Synthesis, structure-activity relationships, and in vivo efficacy of the novel potent and selective anaplastic lymphoma kinase (ALK) inhibitor 5-chloro-N2-(2-isopropoxy-5-methyl-4-(piperidin-4-yl)phenyl)-N4-(2-(isopropylsulfonyl)phenyl)pyrimidine-2,4-diamine (LDK378) currently in phase 1 and phase 2 clinical trials, J. Med. Chem. 56 (2013) 5675–5690.

[19] L. Friboulet, N. Li, R. Katayama, C.C. Lee, J.F. Gainor, A.S. Crystal, P.Y. Michellys, M.M. Awad, N. Yanagitani, S. Kim, A.C. Pferdekamper, J. Li, S. Kasibhatla, F. Sun, X. Sun, S. Hua, P. McNamara, S. Mahmood, E.L. Lockerman, N. Fujita, M. Nishio, J.L. Harris, A.T. Shaw, J.A. Engelman, The ALK inhibitor ceritinib overcomes crizotinib resistance in non-small cell lung cancer, Cancer Discov. 4 (2014) 662–673.

[20] S. Dhillon, M. Clark, Ceritinib: first global approval, Drugs 11 (2014) 1285–1291.

[21] W.S. Huang, S. Liu, D. Zou, M. Thomas, Y. Wang, T. Zhou, J. Romero, A. Kohlmann, F. Li, J. Qi, L. Cai, T.A. Dwight, Y. Xu, R. Xu, R. Dodd, A. Toms, L. Parillon, X. Lu, R. AnjuM, S. Zhang, F. Wang, J. Keats, S.D. Wardwell, Y. Ning, Q. Xu, L.E. Moran, Q.K. Mohemmad, H.G. Jang, T. Clackson, N.I. Narasimahan, V.M. Rivera, X. Zhu, D. Dalgarno, W.C. Shakespeare, Discovery of brigatinib (AP26113), a phosphine oxide-containing, potent, orally active inhibitor of anaplastic lymphoma kinase, J. Med. Chem. 59 (2016) 4948–4964.

[22] S. Zhang, R. Anjum, S. Squillace, S. Nadworny, T. Zhou, J. Keats, Y. Ning, S.D. Wardwell, D. Miller, Y. Song, L. Eichinger, L. Moran, W.S. Huang, S. Liu, D. Zou, Y. Wang, Q. Mohemmad, H.G. Jang, E. Ye, N. Naraimhan, F. Wang, J. Miret, X. Zhu, T. Clackson, D. Dalgarno, W.C. Shakespeare, V.M. Rivera, The potent ALK inhibitor brigatinib (AP26113) overcomes mechanisms of resistance to first- and second-generation ALK inhibitors in preclinical models, Clin. Cancer Res. 22 (2016) 5527–5538.

[23] A. Markham, Brigatinib: first global approval, Drugs 10 (2017) 1131–1135.

[24] L. Mezquita, D. Planchard, The role of brigatinib in crizotinib-resistant non-small cell lung cancer, Cancer Manag. Res. 10 (2018) 123–130.

[25] K. Kinoshita, K. Asoh, N. Furuichi, T. Ito, H. Kawada, S. Hara, J. Ohwada, T. Miyagi, T. Kobayashi, K. Takanashi, T. Tsukaguchi, H. Sakamoto, T. Tsukuda, N. Oikawa, Design and synthesis of a highly selective, orally active and potent anaplastic lymphoma kinase inhibitor (CH5424802), Bioorg. Med. Chem. 20 (2012) 1271–1280.

[26] H. Sakamoto, T. Tsukaguchi, S. Hiroshima, T. Kodama, T. Kobayashi, T.A. Fukami, N. Oikawa, T. Tsukuda, N. Ishii, Y. Aoki, CH5424802, a selective ALK inhibitor capable of blocking the resistant gatekeeper mutant, Cancer Cell 19 (2011) 679–690.

[27] J. Paik, S. Dhillon, Alectinib: a review in advanced, ALK-positive NSCLC, Drugs 78 (2018) 1247–1257.

[28] H.Y. Zou, L. Friboulet, D.P. Kodack, L.D. Engstrom, Q. Li, M. West, R.W. Tang, H. Wang, K. Tsaparikos, J. Wang, S. Timofeevski, R. Katayama, D.M. Dinh, L. Lam, J.L. Lam, S. Yamazaki, W. Hu, B. Patel, D. Bezwada, R.L. Frias, E. Lifshits, S. Mahmood, J.F. Gainor, T. Affolter, P.B. Lappin, H. Gukasyan, N. Lee, S. Deng, R.K. Jain, T.W. Johnson, A.T. Shaw, V.R. Fantin, T. Smeal, PF-06463922, an ALK/ROS1 inhibitor, overcomes resistance to first and second generation ALK inhibitors in preclinical models, Cancer Cell 28 (2015) 70–81.

[29] S. Basit, Z. Ashraf, K. Lee, M. Latif, First macrocyclic 3rd-generation ALK inhibitor for treatment of ALK/ROS1 cancer: clinical and designing strategy update of lorlatinib, Eur. J. Med. Chem. 134 (2017) 348–356.

[30] J. Yang, W. Gong, Lorlatinib for the treatment of anaplastic lymphoma kinase-positive non-small cell lung cancer, Expert Rev. Clin. Pharmacol. 12 (2019) 173–178.

[31] S.H. Ignatius Ou, M. Azada, D.J. Hsiang, J.M. Herman, T.S. Kain, C. Siwak-Tapp, C. Casey, J. He, S.M. Ali, S.J. Klempner, V.A. Miller, Next-generation sequencing reveals a Novel NSCLC ALK F1174V mutation and confirms ALK G1202R mutation confers high-level resistance to alectinib (CH5424802/RO5424802) in ALK-rearranged NSCLC patients who progressed on crizotinib, J. Thorac. Oncol. 9 (2014) 549–553.

[32] J. Chen, C. Jiang, S. Wang, LDK378: a promising anaplastic lymphoma kinase (ALK) inhibitor, J. Med. Chem. 56 (2013) 5673–5674.

[33] Q. Huang, T.W. Johnson, S. Bailey, A. Brooun, K.D. Bunker, B.J. Burke, M.R. Collins, A.S. Cook, J.J. Cui, K.N. Dack, J.G. Deal, Y.L. Deng, D. Dinh, L.D. Engstrom, M. He, J. Hoffman, R.L. Hoffman, P.S. Johnson, R.S. Kania, H. Lam, J.L. Lam, P.T. Le, Q. Li, L. Lingardo, W. Liu, M.W. Lu, M. McTigue, C.L. Palmer, P.F. Richardson, N.W. Sach, H. Shen, T. Smeal, G.L. Smith, A.E. Stewart, S. Timofeevski, K. Tsaparikos, H. Wang, H. Zhu, J. Zhu, H.Y. Zou, M.P. Edwards, Design of potent and selective inhibitors to overcome clinical anaplastic lymphoma kinase mutations resistant to crizotinib, J. Med. Chem. 57 (2014) 1170–1187.

[34] J.J. Cui, M. Tran-Dubé, H. Shen, M. Nambu, P.-P. Kung, M. Pairish, L. Jia, J. Meng, L. Funk, I. Botrous, M. McTigue, N. Grodsky, K. Ryan, E. Padrique, G. Alton, S. Timofeevski, S. Yamazaki, Q. Li, H. Zou, J. Christensen, B. Mroczkowski, S. Bender, R.S. Kania, M.P. Edwards, Structure based drug design of crizotinib (PF-02341066), a potent and selective dual inhibitor of mesenchymal-epithelial transition factor (c-MET) kinase and anaplastic lymphoma kinase (ALK), J. Med. Chem. 54 (2011) 6342–6363.

[35] P.D. de Koning, D. McAndrew, R. Moore, I.B. Moses, D.C. Boyles, K. Kissick, C.L. Stanchina, T. Cuthbertson, A. Kamatani, L. Rahman, R. Rodriguez, A. Urbina, A. Sandoval, P.R. Rose, Fit-for-purpose development of the enabling route to Crizotinib (PF-02341066), Org. Process Res. Dev. 15 (2011) 1018–1026.

[36] W. Wang, Y. Diao, W. Li, Y. Luo, T. Yang, Y. Zhao, T. Qi, F. Xu, X. Ma, H. Ge, Y. Liang, Z. Zhao, X. Liang, R. Wang, L. Zhu, H. Li, Y. Xu, Design, synthesis and structure-activity relationship study of aminopyridine derivatives as novel inhibitors of Janus kinase 2, Bioorg. Med. Chem. Lett 29 (2019) 1507–1513.

[37] D. Zhang, X. Zhang, J. Ai, Y. Zhai, Z. Liang, Y. Wang, Y. Chen, C. Li, F. Zhao, H. Jiang, M. Geng, C. Luo, H. Liu, Synthesis and biological evaluation of 2-amino-5-aryl-3-benzylthiopyridine scaffold based potent c-Met inhibitors, Bioorg. Med. Chem. 21 (2013) 6804–6820.

[38] D. Zhang, J. Ai, Z. Liang, C. Li, X. Peng, Y. Ji, H. Jiang, M. Geng, C. Luo, H. Liu, Discovery of novel 2-aminopyridine-3-carboxamides as c-Met kinase inhibitors, Bioorg. Med. Chem. 20 (2012) 5169–5180.

[39] S.J. Tremont, L.F. Lee, H.-C. Huang, B.T. Keller, S.C. Banerjee, S.R. Both, A.J. Carpenter, C.-C. Wang, D.J. Garland, W. Huang, C. Jones, K.J. Koeller, S.A. Kolodziej, J. Li, R.E. Manning, M.W. Mahoney, R.E. Miller, D.A. Mischke, N.P. Rath, T. Fletcher, E.J. Reinhard, M.B. Tollefson, W.F. Vernier, G.M. Wagner, S.R. Rapp, J. Beaudry, K. Glenn, K. Regina, J.R. Schuh, M.E. Smith, J.S. Trivedi, D.B. Reitz, Discovery of potent, nonsystemic apical sodium-codependent bile acid transporter inhibitors (Part 1), J. Med. Chem. 48 (2005) 5837–5852.

[40] J. Li, X. Zhang, Z. Zhang, P.K. Padakanti, H. Jin, J. Cui, A. Li, D. Zeng, N. Rath, H. Flores, J.S. Perlmutter, S.M. Parsons, Z. Tu, Heteroaromatic and aniline derivatives of piperidines as potent ligands for vesicular acetylcholine transporter, J. Med. Chem. 56 (2013) 6216–6233.

[41] X. Hao, Z. Xu, H. Lu, X. Dai, T. Yang, X. Lin, F. Ren, Mild and regioselective N-alkylation of 2-pyridones in water, Org. Lett. 17 (2015) 3382–3385.

[42] A.S.L. Tripos Associates, MO63144, in: SYBYL-X Molecular Modeling Software Package, 2011, version 1.3.

[43] G. Jones, P. Willett, R.C. Glen, A.R. Leach, R. Taylor, Development and validation of a genetic algorithm for flexible docking, J. Mol. Biol. 267 (1997) 727–748.